1971

Thermal lattice expansion of various types of solids

Jayantkumar Shantilal Shah

THERMAL LATTICE EXPANSION OF VARIOUS TYPES OF SOLIDS

by

JAYANTKUMAR SHANTILAL SHAH, 1944-

A DISSERTATION

Presented to the Faculty of the Graduate School of the

UNIVERSITY OF MISSOURI-ROLLA

In Partial Fulfillment of the Requirements for the Degree

DOCTOR OF PHILOSOPHY

in

METALLURGICAL ENGINEERING

1971

M. E. Straumanis
(Advisor)

W. J. James

J. B. Clark

William A. Tiedad

Tetsuro Suzuki

ABSTRACT

Thermal lattice expansion studies of various types of solids were carried out in this investigation and were corelated to their crystallographic and various other properties. The advantages and limitations of various methods of studying thermal expansion are discussed in detail A new design for a versatile low temperature camera to study expansion by an X-ray method is proposed.

The thermal lattice expansion of silicon was negative below 119^{o}K. This behavior is discussed in terms of crystal structure and interatomic bonding. Diamond exhibits no anomalous thermal expansion.

Lattice parameter data for many metals at low temperatures are reported for the first time. The thermal expansion behavior of Fe, Cu, Ni, W and Cr is typical for metals. A large difference between the present results and the published data (obtained by measuring bulk expansion) was observed for tungsten. This is explained in terms of the lack of a theoretical density for the bulk samples. Tungsten and chromium show no thermal expansion anomalies despite the theoretical predictions and some indirect evidence. The small magnitude of the thermal expansion of $A\ell_2Au$ is discussed in terms of the interatomic bonding in the structure.

LiF shows constant values of Gruneisen parameters at unusually high temperatures.

The thermal expansion behavior of magnetic intermetallic compounds such as R_2M_{17} (R=Y,Lu,Gd and M=Fe,Co,Ni) is clearly corelated to their magnetic properties and crystallographic structures. An anomalous thermal expansion in the c direction is found for R_2Fe_{17} compounds below their magnetic ordering temperatures. This is explained in terms of the Fe-Fe interatomic distances and number of Fe nearest neighbors in the crystal. No such anomalous behavior is found for the isostructural R_2Co_{17} or R_2Ni_{17} compounds. The ferromagnetic to helimagnetic transition in Lu_2Fe_{17} can be understood as due to negative direct interactions and stored magnetic energy in the substitution zone.

ACKNOWLEDGEMENT

The author would like to express his sincere gratitude to Dr. M. E. Straumanis, Professor of Metallurgy and Senior Investigator at the Graduate Center for Materials Research, for his constant direction, patient consultation and sincere interest throughout the course of this investigation.

He would also like to thank Dr. W. J. James, Professor of Chemistry and Director of the Graduate Center for Materials Research and Dr. R. Lemaire, Visiting Professor of Metallurgical Engineering, for their continued interest and Mrs. Phyllis Smith for her help in the typing department.

The work on magnetic solids in this investigation was only possible due to the close collaboration with the Laboratoire d'Electrostatique et Physique du Métal, Grenoble - France.

The author is thankful for the financial aid received from the University of Missouri-Rolla. Part of this work was supported by a grant from Air Force Materials Laboratories in Dayton, Ohio.

TABLE OF CONTENTS

Page

LIST OF TABLES

LIST OF FIGURES

I. INTRODUCTION

An accurate knowledge of the temperature dependence of thermal expansion of solids at low temperatures provides a better understanding of the equation of state of solids. In the Grüneisen[1] theory of thermal expansion, the Grüneisen parameter, γ, is defined by

$$\gamma = 3\alpha V K_T/C_V \tag{1}$$

where α is the coefficient of linear thermal expansion, K_T is the isothermal bulk modulus, C_V the heat capacity at constant volume, and V the molar volume. The Grüneisen parameter was originally regarded as a constant, independent of temperature and lattice vibrational frequency. This simple picture turned out to be inadequate for real solids. Theoretical works of Barron[2] and Blackman[3] have shown that variations in the values of γ are to be expected at temperatures below 0.2 θ, where θ is the Debye characteristic temperature.

It was also shown recently that at low temperatures, the electronic contributions[4] of metals and magnetic contributions of magnetic solids to the total thermal expansion can dominate over the lattice contributions. The former are easily separable from the latter. This in turn yields a better picture of these types of solids.

There are many data available on the thermal expansion of solids near room temperature and at high temperatures,

but they are scanty and inconsistent at low temperatures. Most of the existing data below room temperature has been obtained by dilatometric methods which use bulk samples and liquid gases, allowing only the study of macroscopic (bulk) thermal expansion (length changes). The use of macroscopic polycrystalline samples in such methods introduces errors in the expansivity, $(\Delta\ell/\ell)$, measurements due to microvoids, microcracks, grain boundaries, etc., and oxide layers. In contrast, the lattice expansion measurements by X-ray diffraction techniques are independent of such errors. In a few cases, appreciable differences in thermal expansivity between the two methods have been reported, amounting to about ten percent at the most.[6-9]

There is a lack of extensive lattice parameter data at low temperatures because the previous cryogenic X-ray diffraction cameras needed very elaborate cooling systems, utilizing a series of Dewar vessels containing dry ice (in acetone), liquid oxygen, nitrogen, hydrogen, and helium.[10-12] This type of setup in metal cryostats presents numerous design and experimental difficulties. With the advent of the closed cycle refrigerating systems using the Joule-Thompson effect, these difficulties are minimized since no liquid gases are needed. A recent design of a symmetrical back-reflection focusing camera by Woodard and Straumanis[13] connected with a Joule-Thompson pump has shown this to be true.

In the view of the above facts, the present investigation consisted of studies of lattice parameters, thermal expansion coefficient, and Grüneisen parameters of various types of solids. These were studied according to the following outline.

A. Substances with a Diamond Cubic-Type Structure:

Solids possessing a diamond cubic or zincblende type lattice generally exhibit negative thermal expansion behavior at very low temperatures. Silicon and diamond were selected to observe this phenomenon.

1. Silicon exhibits a negative thermal expansion below 120°K. These results were also used to compare the precision of temperature control and thermal expansion obtained by our X-ray diffraction method (without using liquid gases) with a dilatometric method[10] employing liquid gases.
2. Diamond is thought of as having a constant thermal expansion over the entire temperature range without any anomalies. Therefore, diamond was studied to check the above notion and the recent theoretical predictions[14] that diamond should show a negative thermal expansion at low temperatures.

B. Metals, Intermetallic Compound Al_2Au and LiF:

For most metals, the thermal expansion coefficients and Grüneisen parameters decrease with temperature. With this in mind, chromium, tungsten, iron, copper and

nickel were studied at low temperatures.

1. On the basis of compressibility data, an anomaly in the thermal expansion of Cr was predicted at $120^{o}K$.[15] Chromium was selected for this reason.
2. As for tungsten, all existing thermal expansion data were obtained on sintered bulk samples. As our X-ray method uses a powder sample, there was a further possibility to compare the results obtained by two different methods employing two different types of samples.
3. Iron samples of various degrees of purity were studied to observe the effects of impurities on the thermal expansion.
4. Copper and nickel were included in the present investigation since no precise low temperature lattice parameter data are available for them.
5. $A\ell_2Au$ was selected for studies to state whether or not such a compound resembles a metal in its thermal expansion behavior.
6. LiF was studied since no accurate lattice parameters of LiF were available when this investigation was started. Secondly, there was some doubt as regards its low temperature limit of the Grüneisen parameter.

C. Magnetic Intermetallic Compounds:

The thermal variation of lattice parameters of magnetic intermetallic compounds such as Lu_2Fe_{17},

α-Gd_2Fe_{17}, Y_2Co_{17}, Y_2Ni_{17} having an hexagonal Th_2N_{17}-type structure, β-Gd_2Fe_{17} of rhombohedral Th_2Zn_{17}-type structure, and YCo_5, YNi_5 of hexagonal $CaCu_5$-type structure were studied in the temperature range 25°-900°K. The primary reasons for this study were the following:

i) To understand what really determines the magnetic properties, structure and stability of these compounds and how are they affected by the following parameters:
   a) the interatomic distances between the transition metal atoms and temperature,
   b) the size of the atomic radius, particularly in structures of the Th_2Ni_{17}-type, and
   c) the conduction electron transfer from the rare earth or yttrium atoms to the transition metals.

ii) To observe the thermal expansion behavior of A_2B_{17} (A=Lu,Gd,Y; B=Fe,Co,Ni) Th_2Ni_{17}-type isostructural intermetallic compounds. Do they all show a typical behavior or not? Since the $CaCu_5$-type structure is the building block of Th_2Ni_{17}-type structure, the thermal expansion behavior of YCo_5 and YNi_5 was studied.

iii) To observe the thermal expansion behavior of α and β polymorphs of Gd_2Fe_{17} intermetallic compound. The only difference between the α and β forms of

this compound is in the type of substitutional ordering; for the former it is of the type AB AB... Whereas for the latter it is ABC ABC ...

iv) For Lu_2Fe_{17}, there is evidence in the literature that it shows a hysteresis in its thermal magnetization behavior.[16] Our intention was to see whether a similar hysteresis exists for this compound in the thermal variation of its lattice parameters.

D. Studies Toward Development of a Better and More Versatile X-ray Camera:

Due to certain limitations in the present low temperature X-ray camera used in this investigation, a detailed study was made of the existing X-ray cameras and refrigerating systems to design a more versatile low temperature camera. A new design is proposed.

II. GENERAL THEORY OF THERMAL EXPANSION AND GRÜNEISEN PARAMETERS OF SOLIDS AT LOW TEMPERATURES

A. Thermal Expansion:

The atoms in a crystal are constantly executing vibrations about their equilibrium positions. When the crystal is further heated, the amplitude of their vibrations increases. If these vibrations were perfectly harmonic, the crystal would show no thermal expansion. Such a perfectly harmonic crystal is mechanically unstable and no such crystals exist. So it is the anharmonicity of these vibrations that brings about the expansion of a crystal.

The coefficient of the linear thermal expansion of crystals is defined as

$$\alpha_T = \frac{1}{\ell_T} \left(\frac{\partial \ell}{\partial T}\right)_P . \tag{2}$$

where T denotes the temperature of the crystal and ℓ_T its length at that temperature. A similar definition holds for the volume expansion coefficient, β, for the crystal.

$$\beta = \frac{1}{V_T} \left(\frac{\partial V}{\partial T}\right)_P \tag{3}$$

For the cubic crystals, to a first degree of approximation, $\beta=3\alpha$.

B. Grüneisen Parameters:

Grüneisen[1] has shown that β, the volume expansion coefficient for a Debye solid, should be approximately proportional to the specific heat at constant volume, C_V. Since the latter is proportional to T^3 for a Debye solid; β also has a T^3 dependence. Grüneisen has developed a simple relationship between β and some other thermodynamic properties.

$$\beta/\chi_T = \gamma C_V/V \tag{4}$$

where χ_T is the isothermal compressibility,

$$\chi_T = - 1/V \cdot (\partial V/\partial P)_T \tag{5}$$

V is the molar volume and γ is the Grüneisen parameter. β is also related to the Helmholtz free energy A or entropy S of the system as follows (Eqs. 3 and 5)

$$\beta/\chi_T = - \left(\frac{\partial V}{\partial T}\right)_P / \left(\frac{\partial V}{\partial P}\right)_T = \left(\frac{\partial P}{\partial T}\right)_V \tag{6}$$

From Maxwell's relations,

$$\left(\frac{\partial P}{\partial T}\right)_V = \left(\frac{\partial S}{\partial V}\right)_T = - \frac{\partial^2 A}{\partial V \partial T} \tag{7}$$

$$\therefore \beta/\chi_T = \left(\frac{\partial S}{\partial V}\right)_T = - \frac{\partial^2 A}{\partial V \partial T} \tag{8}$$

Mott and Jones[17] have shown that Eq. (4), the Grüneisen relation, can also be obtained from Eq. (8). Then the

Grüneisen parameter is,

$$\gamma = - \partial \log \omega / \partial \log V \qquad (9)$$

That is, the change in vibrational frequencies, ω of atoms in a solid with the volume, V. In his theory, Grüneisen assumed that d log ω/d log V is the same for all frequencies of the solid. Accordingly, γ, the Grüneisen parameter, is independent of temperature. The Grüneisen parameter was assumed to be constant for most solids at least down to temperatures as low as 1/5 θ, where θ is the Debye characteristic temperature. However, accurate measurements of β have shown that γ varies with temperature at and below 1/10 θ. The Grüneisen parameter would be constant if all the atoms in the solid would vibrate independently of each other with a single frequency (Einstein model) or if the volume dependence of the frequency would be the same for all vibrations (Debye model). Variation of γ with temperature indicates that various frequency spectra depend differently on volume.

It can also be said that the thermal expansion is the result of anharmonic contributions to the crystal potential energy. Since we know very little about the specific values of anharmonic terms in a particular lattice, the problem can be treated by a quasi-harmonic approximation, neglecting the anharmonic terms, but permitting the interaction constants of the harmonic

theory to become volume dependent. As previously shown

$$\beta/\chi_T = (\partial S/\partial V)_T = - \partial^2 A/\partial V \partial T \qquad (10)$$

which relates the thermal expansion to changes in entropy S or to the Helmholtz free energy A of the system. The formulation embraces contributions to thermal expansion not only from the lattice but also from conduction electrons, and from magnetic interactions. For the present discussion, we are only concerned with the lattice; other contributions will be treated in the next section. In the quasi-harmonic approximation, the lattice of N ions is represented by a system of 3N loosely coupled harmonic oscillators. The free energy of the system is then

$$A(V,T) = \underset{\substack{\uparrow \\ \text{configurational} \\ \text{energy}}}{U(V)} + \underset{\substack{\uparrow \\ \text{zero point} \\ \text{energy}}}{\sum_{i=1}^{3N} \tfrac{1}{2}\hbar\omega_i(V)} + kT \underset{\substack{\uparrow \\ \text{thermal} \\ \text{energy}}}{\sum_{i=1}^{3N} \ell n(1-e^{-\hbar\omega_i/kT})} \qquad (11)$$

where ω_i is the frequency of the $i^{\underline{th}}$ lattice mode. The Grüneisen relation, Eq. (4),

$$\beta/\chi_T = \gamma C_V/V$$

follows also from Eqs. (10) and (11) if

$$\gamma_T = \sum_{i=1}^{3N} \gamma_i C_i \Big/ \sum_{i=1}^{3N} C_i \qquad (12)$$

Here

$$\gamma_i = - (d \log \omega_i / d \log V)_T$$

and C_i are the contributions to the specific heat, C_V, from the $i^{\underline{th}}$ mode.

$$C_i = k\left(\frac{\hbar\omega_i}{kT}\right)^2 \frac{\exp(\hbar\omega_i/kT)}{[\exp(\hbar\omega_i/kT)-1]^2} \tag{13}$$

At high temperatures ($T>>>\theta$), all modes contribute equally to the specific heat and $\gamma=\gamma_\infty$ is the simple average

$$\gamma_\infty = \frac{1}{3N} \sum_{i=1}^{3N} \gamma_i \text{ for } T>>\theta \tag{14}$$

So, for most solids, γ is approximately constant at high temperatures with a numerical value of about two. At very low temperatures ($T<<<\theta$), where only the acoustic waves are important, γ approaches a limiting value.

$$\gamma_o = \sum_{i=1}^{3N} \gamma_i \nu_i^{-3} \Big/ \sum_{i=1}^{3N} \nu_i^{-3} (T<<<\theta) \tag{15}$$

where ν_i is the velocity of the $i^{\underline{th}}$ mode.

The amount of variation in the Grüneisen parameter $(\gamma_\infty-\gamma_o)$ depends on the structure of the material and on the nature of the interactions between the particles.

C. Electronic and Magnetic Contributions to the Thermal Expansion:

The total thermal expansion can be separated in terms of β_ℓ (lattice), β_e (electronic) and β_m (magnetic). For the free energy of the system in Eq. (11), we have considered only the configurational, zero point and lattice vibrational energies. But for metals and magnetic solids, we can easily visualize additional terms to the total free energy of the system due to the conduction electrons (in metals) and magnetic interaction energy for the magnetic solids. Similarly, we have entropy contributions due to lattice (dS_ℓ), conduction electrons (dS_e) and magnetic interactions (dS_m). Then Eq. (10) can be rewritten as

$$(\beta_\ell+\beta_e+\beta_m)/\chi_T = \left(\frac{\partial S_\ell}{\partial V}\right)_T + \left(\frac{\partial S_e}{\partial V}\right)_T + \left(\frac{\partial S_m}{\partial V}\right)_T \qquad (16)$$

1. Electronic thermal expansion for metals:

The conduction electrons in a metal give rise to considerable expansion at very low temperatures.[18] This can be interpreted by a simple kinetic picture as a change in volume of the lattice required to maintain a constant electron "pressure" when the temperature changes. This gives rise to an electronic thermal expansion β_e which can be expressed in terms of electronic specific heat, C_e,

and electronic Grüneisen parameter, γ_e, as

$$\beta_e/\chi_T = \gamma_e \, C_e/V \tag{17}$$

At very low temperatures, the electronic specific heat, C_e, decreases linearly with temperature and it dominates over the lattice specific heat ($C_e >>> C_\ell$). Therefore, at such low temperatures, the thermal expansion is almost entirely due to the conduction electrons. Since the electronic specific heat, C_e, decreases linearly with temperature, the electronic thermal expansion β_e also decreases linearly with temperature.

2. Magnetic thermal expansion for magnetic solids:

For magnetic solids, entropy, S_m, is contributed by magnetic interactions; and it gives rise to the magnetic thermal expansion, β_m. If the magnetic entropy is expressed in terms of $F(E_m/T)$, where E_m is the magnetic interaction energy, then β_m can be related to magnetic specific heat, C_m, by a "magnetic Gruneisen parameter", γ_m[19]

$$\beta_m/\chi_T = \gamma_m \, C_m/V \tag{18}$$

where

$$\gamma_m = (-d \log E_m/d \log V) \tag{19}$$

In view of these lattice, electronic and magnetic contributions to the thermal expansion,

$$\beta_{Total}/\chi_T = (C_\ell\gamma_\ell + C_e\gamma_e + C_m\gamma_m)/V \qquad (20)$$

III. EXPERIMENTAL

For the low temperature lattice expansion studies, a symmetrical back-reflection, focusing camera designed by Woodard[20] was used. Here, the cooling is accomplished without liquid gases by a Joule-Thompson pump.

A. Sample Calculations for Lattice Parameter Determination:

The distance L between a pair of diffraction lines centered on the slit opening in a back-reflection camera is given by

$$L = 4R(\pi - 2\theta) \tag{21}$$

where R is the radius of the film cylinder, and θ is one-half of the angle between the primary X-ray beam and the diffracted line. Solving Eq. (21) for the angle gives

$$\theta = (\pi/2) - (L/8R) \tag{22}$$

Determination of θ in degrees for the following values

$$\pi = 3.14159 \text{ radians}$$
$$1 \text{ radian} = 57.2958 \text{ degrees}$$
$$R = 36.5126 \text{ mm}$$

gives

$$\theta^{o} = 90.0 - 0.196151\ L \tag{23}$$

where the constant 0.196151 was determined from the

radius of the film cylinder used in the investigation. Data for the sample calculation refer to the room temperature film for Lu_2Fe_{17} hexagonal intermetallic compound. For the hexagonal lattice, the position of a line having the indices hkℓ, is determined by two parameters, a and c. It is impossible to calculate both of them from the observed position of a single line alone. Positions of two independent lines are required. In the hexagonal system, the value of d, the distance between adjacent planes in the set (hkℓ), is found from the equation:

$$\frac{1}{d^2} = \frac{4}{3}\left(\frac{h^2+hk+k^2}{a^2}\right) + \frac{\ell^2}{c^2} \qquad (24)$$

combining this with the Bragg's Law

$$n\lambda = 2d\sin\theta \qquad (n=1)$$

$$\text{or} \quad \lambda^2 = 4d^2\sin^2\theta$$

and substituting for $d^2=\frac{\lambda^2}{4\sin^2\theta}$ in Eq. (24), we obtain

$$\sin^2\theta = \frac{\lambda^2}{4}\left[\frac{4}{3} \cdot \frac{(h^2+hk+k^2)}{a^2} + \frac{\ell^2}{c^2}\right] \qquad (25)$$

For Lu_2Fe_{17} two high angle reflections were observed. Cr radiation was used. Cr K_{α_1} $\lambda=2.28962$ Å and $\lambda^2=5.2423597$.

TABLE I

SAMPLE CALCULATIONS FOR Lu_2Fe_{17}

Line	(600)	(306)
L (mm)	L_1=95.75	L_2=92.35
$\theta^o=90^o-0.196151L$	θ_1=71.218542	θ_2=71.885455
$Sin^2\theta$	$Sin^2\theta_1$=0.89634219	$Sin^2\theta_2$=0.903330175

When the above data are substituted in Eq. (25), we obtain two simultaneous equations which can be solved for the two unknowns, a and c, in the following way. For the (600) reflection:

$$Sin^2\theta_1 = \frac{\lambda^2}{4}\left[\frac{4}{3} \cdot \frac{36}{a^2}\right] \tag{26}$$

So,

$$a^2 = \frac{12\lambda^2}{Sin^2\theta_1} \tag{27}$$

Taking from Table I the value of $Sin^2\theta_1$, using Eq. (27), a parameter was found

$$a = 8.37755 \text{ Å}$$

Substituting the Eq. (27) in Eq. (25) for a^2 and simplifing it, we find:

$$c^2 = \frac{36\ \lambda^2}{4Sin^2\theta_2 - Sin^2\theta_1} \tag{28}$$

Knowing the values of $Sin^2\theta_1$ and $Sin^2\theta_2$ from Table I, the $\underline{c}$ parameter was found

$$\underline{c} = 8.33435 \text{ Å}$$

B. Refraction Corrections:

The refraction of X-rays in a solid results from a change in wavelength in it, and, hence, also in the Bragg angle, θ. This causes an apparent change in the spacing. For high precision, the directly measured values of lattice parameters should be corrected for refraction by adding to it a correction.[21] For cubic substances, the formula is quite simple[22]

$$a(1-n) = 4.47 \times 10^{-6}(\lambda/a)^2 \Sigma Z \qquad (29)$$

where a is the directly measured lattice parameter, a(1-n) the refraction correction, n the coefficient of X-ray refraction, λ the wavelength of radiation used, and ΣZ is the sum of the atomic numbers of the atoms in the unit cell.

For diamond, the directly measured lattice parameter is 3.56699 Å, which was obtained by using Co K_β (λ=1.62050 Å) radiation and the (331) lines. So to obtain the refraction correction, we use the Eq. (29)

λ = 1.62050 Å
a = 3.56699 Å
ΣZ = 8 atoms/unit cell x 6 (atomic number of c)
= 48
a(1-n) = .000044 Å

For the absolute values of lattice parameters, this correction is absolutely necessary, but for the precise thermal expansion studies, it is not needed since this refraction correction is temperature independent and thermal expansion coefficient only involves a rate of change of lattice parameter with temperature, da/dT. So by neglecting the refraction correction in the thermal expansion coefficient calculations, one simply omits a systematic error.

C. Proof of the Very Precise Temperature Control in the Low Temperature Camera:

The platinum resistance sensor was used to measure and control the temperature, and this sensor was calibrated against another sensor by the Kelvin bridge. In spite of these calibrations, there was some doubt as regards the temperature of the sample itself. Therefore, the parameters obtained were compared with those obtained by other workers who had used liquid gases in their camera for cooling.[10] The lattice parameters of silicon obtained in this investigation were, therefore, carefully checked against those measured by Batcheder and Simmons. From Fig. 1 and Table II, it is evident that the lattice parameters obtained by our method agree very well with those found in a different laboratory, by a different method, different temperature calibrations and measurement procedures. This agreement in turn confirms the accuracy of the temperature

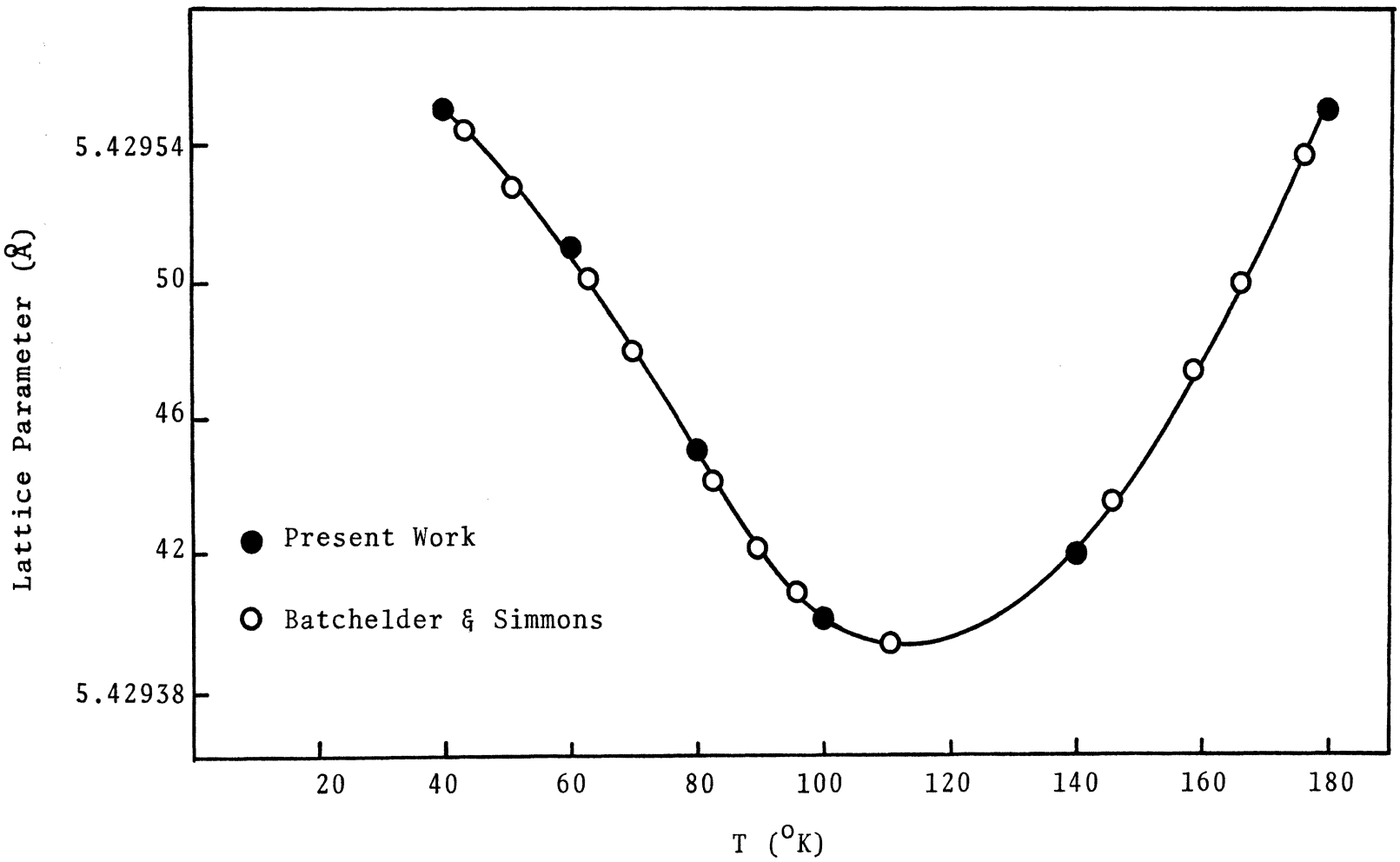

FIGURE 1. Lattice parameters of silicon

measurement and control of the temperature in our low temperature camera. The temperature of the sample is the same as shown by the temperature measuring devices.

TABLE II

THE COMPARISON OF LATTICE PARAMETERS OF SILICON

[.00004 Å refraction correction added, $CuK\alpha_1$=1.54051 Å, (444) line]

T^oK	Present Work (Å)	Batchelder and Simmons* (Å)
180	5.42955	5.42955
140	5.42942	5.42941
100	5.42940	5.42938
80	5.42945	5.42947
60	5.42951	5.42949
40	5.42955	5.42955

* Calculated from ($\Delta a/a'$) where a'=5.43044 Å at 273.15°K

D. Check of the Uniformity of the Film Cylinder Radius Throughout Its Whole Height:

The low temperature camera used in this investigation utilizes a multi-exposure technique on a single film. The film cylinder of it can be moved along a directing steel cylinder. Both of these were machined very precisely, but a check of the uniformity of the film cylinder was necessary. For this purpose six exposures of diamond powder on a single film cylinder

were made at room temperature (298·20°K±.05), and the lattice parameters were calculated by measuring the (331) β lines of each exposure. These results are shown in Table III.

TABLE III

LATTICE PARAMETERS OF DIAMOND AT 298.20°K OBTAINED ON ONE FILM IN SIX CONSECUTIVE EXPOSURES*

Film Position	Lattice Parameter Å
A	3.56699
B	3.56699
C	3.56698
D	3.56698
E	3.56698
F	3.56697

* Co K_β (λ=1.62075 Å), (331) β line, not corrected for refraction

The above results indicate that the film radius or radius of the film holder is uniform for all the six exposures for the entire height of the film.

E. Lattice Expansion Studies in the Vicinity of Room Temperature and Up to 900°K

For temperatures in the vicinity of room temperature, the lattice expansion studies were made in a Straumanis camera with asymmetric film loading.

Temperatures higher and lower than room temperature were obtained by circulating hot and cold mixtures of water and anti-freeze in a properly insulated aluminum jacket surrounding the camera. Temperature was measured by a thermometer capable of $\pm.05^{o}K$ in precision. The lowest temperature obtained in this arrangement was $250^{o}K$, and the highest was $335^{o}K$. It was not possible to go much higher in this experimental setup since the film also is at the same temperature and above $345^{o}K$ the film begins to blacken throughout during the development. The powder samples were mounted on a thin quartz fiber with the aid of vaseline.

For temperatures higher than $335^{o}K$ and up to $900^{o}K$, a Rigaku-Denki high temperature camera was used where the film remained at room temperature. The quality of films obtained in this camera as received was very poor because the exposure times were too long due to the thick nickel heat shields. These were replaced by thin foils of aluminum. The camera was also re-designed to obtain larger 2θ values in the back-reflection region. The asymmetric film placement could be used with this camera. However, there was still the question of temperature calibration. Since a precise measurement of lattice parameters of gold is available as a function of temperature[23] (up to $1300^{o}K$), it was decided to use gold for the temperature calibration. The powder samples were sealed in quartz capillaries under vacuum to prevent oxidation.

F. Thermal Expansion Coefficients and Grüneisen Parameters:

Thermal expansion coefficients, α, were calculated by using Eq. (2). The lattice parameters were plotted on large graph papers (75x90 cm) as a function of temperature and tangents were drawn at appropriate temperatures. To obtain α, da/dT from the graphs was divided by the lattice parameter at some reference temperature (usually 273.15°K).

The lattice parameters were also fitted to polynomial equations of various degrees as a function of temperature by means of a linear least squares computer program. From the resulting equation relating the lattice parameters to temperature with the least standard deviation, da/dT was found by differentiation. Thus, if the lattice parameter as a function of temperature is:

$$a(T)\ \text{Å} = A + BT + CT^2 + DT^3 + ET^4 \qquad (30)$$

then the expansivity is:

$$da/dT(T) = B + CT + DT^2 + ET^3 + \ldots \qquad (31)$$

When the desired temperature values are substituted into Eq. (31), da/dT can be calculated for a given temperature. The expansivity values divided by the lattice parameter at some reference temperature then represent the thermal expansion coefficients.

Both graphical and numerical methods produced quite close values of the thermal expansion coefficients.

The Grüneisen parameters were calculated from Eq. (1). The values of thermal expansion coefficients were from this study and those of specific heats and compressibilities were taken from the literature.

IV. LATTICE PARAMETERS, THERMAL EXPANSION COEFFICIENTS AND GRÜNEISEN PARAMETERS OF SUBSTANCES WITH DIAMOND CUBIC-TYPE STRUCTURES IN THE 180°-40°K RANGE: SILICON AND DIAMOND

A. Literature Survey:

1. Silicon

There is only the work of Batchelder and Simmons[10] regarding the lattice parameters of silicon at low temperatures. They have also calculated the thermal expansion coefficients and Grüneisen parameters of the element at low temperatures. The measurements were made on a silicon single crystal (20Ω·cm resistivity) in an X-ray back-reflection, rotating camera. Liquid gases were used for cooling. Film shrinkage and refraction corrections were applied in their lattice parameter measurements at various temperatures, and it was found that the thermal expansion of silicon becomes zero at 117°K and negative upon further cooling.

All the other thermal expansion studies on silicon were made by dilatometric techniques employing bulk samples and liquid gases.

Gibbons[24] has studied the thermal expansion of silicon single crystals in the range of 4.2° to 300°K by an interferometeric method. These measurements show the thermal expansion of silicon to be zero at 120°K and negative below this temperature.

Carr, et al.[25] determined the thermal expansion of a silicon single crystal by a dilatometric method. They found that the thermal expansion of silicon becomes negative below 130°K but to a much smaller extent than reported by Batchelder and Simmons.

2. Diamond

The only X-ray lattice expansion study of diamond is by Thewlis and Davey.[28] They have used a stream of liquid N_2 vapors impinging on the sample mounted in a regular 19 cm Unicam camera. The diamond powder was held in silica capillaries of an internal diameter of 0.5 mm. The authors do not list the accuracy of their temperature measurements. They find that industrial quality diamond shows an anomalous thermal expansion behavior at low temperatures; at 243°K the thermal expansion is zero and below 243°K, slightly negative. No such anomaly was found for gem quality diamond. The shape of their thermal expansion curves appears to be doubtful.

Novikova[29] measured the thermal expansion of two large diamonds by a dilatometric method. Her results indicate that the thermal expansion of diamond becomes zero at 90°K and very slightly negative below it.

Dolling and Cowley[14] predicted from their theoretical calculations that the thermal expansion

of diamond should become negative below 60°K.

B. Experimental Details:

Lattice parameter determinations in the present investigation were made with 99.999% silicon powder obtained from Koch Light Labs, Colnbrook, England. Particle size of 20 microns or less was needed to obtain uniform and sharp diffraction patterns. Three exposures at each of the temperatures of 40°, 60°, 80°, 100°, 140° and 180°K were taken. Lattice parameters were calculated by measuring the distance between the (444) α_1 lines produced by copper $K\alpha_1$ radiation ($\lambda(\alpha_1)$=1.54051 Å).

Lattice parameter determinations for diamond were made with a diamond powder distributed by the International Union of Crystallography-Precision Lattice Parameter Project.[30] An original sample of Congo diamond powder of a crystallite size between 6 and 12μ was used. With Co radiation this powder gave very sharp and uniform lines. Lattice parameters were calculated by measuring the (331) β lines, produced by Co K_β radiation (λ=1.62050 Å). Three exposures at temperatures of 40°, 60°, 80°, 100°, 140° and 180° were taken.

C. Results:

1. Silicon

Lattice parameters of silicon have been already compared with those of Batchelder and Simmons

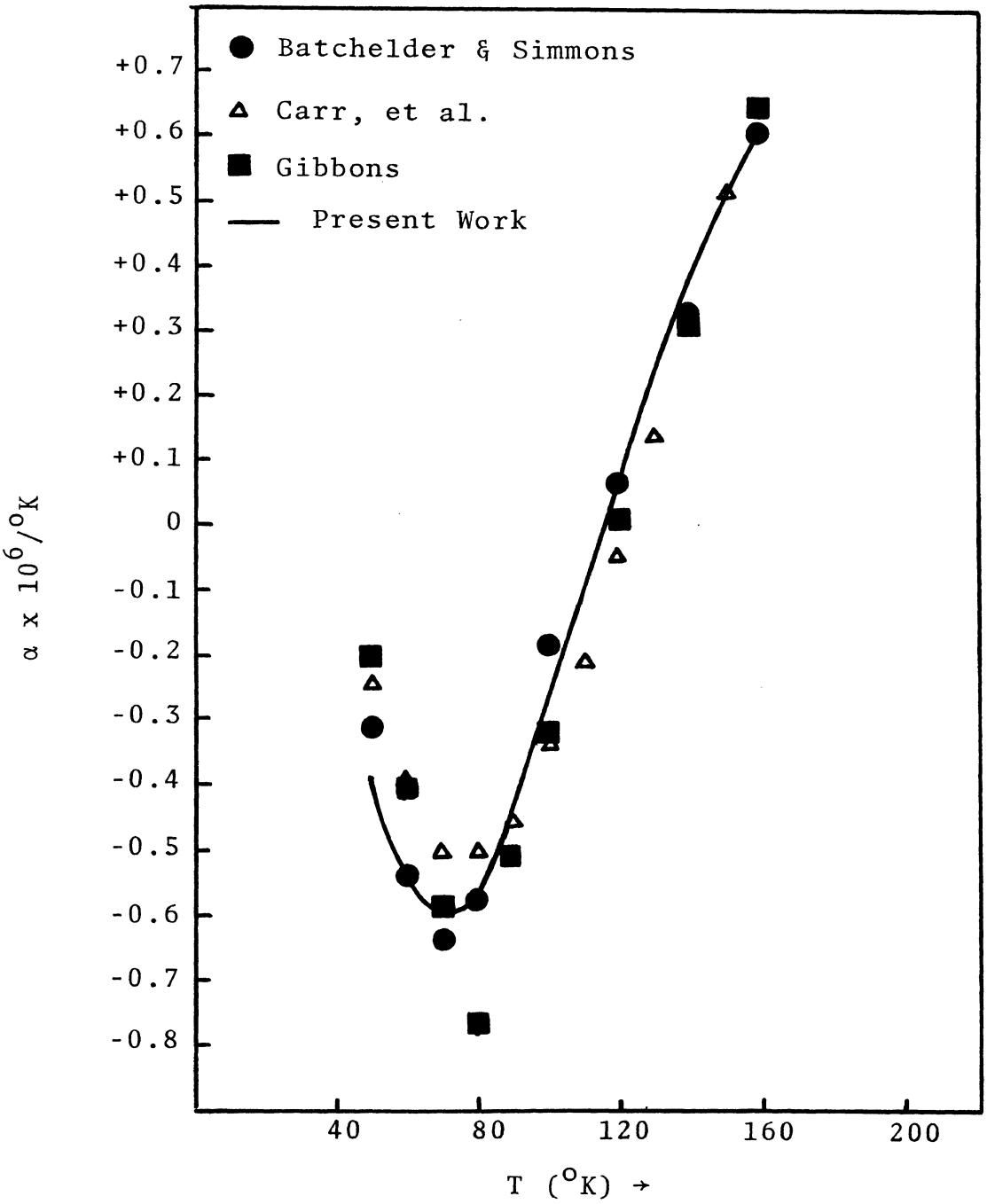

FIGURE 2. Thermal expansion of silicon

(Fig. 1, Table II). Present results are in excellent agreement with theirs. The following equation relates the lattice parameters of silicon as a function of temperature in the range of 40^{o}-180^{o}K.

$$a(T)\text{Å} = 5.42926 + 1.56 \times 10^{-5} T - 3.15 \times 10^{-7} T^2 + 2.15 \times 10^{-9} T^3 - 4.68 \times 10^{-12} T^4 \quad (32)$$

The thermal expansion coefficients, α, were calculated from Eq. (32) by a procedure outlined in Section II. Values of α obtained in the present investigation together with those of Carr, et al., Gibbons and Batchelder and Simmons are shown in Fig. 2 and listed in Table IV. The thermal expansion of silicon becomes zero at 120^{o}K and negative below 120^{o}K. The maximum magnitude of negative thermal expansion is found to be -0.60×10^{-6} at 70^{o}K.

TABLE IV

THERMAL EXPANSION COEFFICIENTS OF SILICON AT LOW TEMPERATURES

	$\alpha \times 10^{6}/^{o}$K			
T^{o}K	Present Results	Carr et al.	Gibbons	Batchelder & Simmons
160	0.63		0.65	0.62
140	0.48		0.31	0.33
120	0.12	-0.04	0.01	0.07

$T^{o}K$	$\alpha x10^{6}/^{o}K$			
	Present Results	Carr et al.	Gibbons	Batchelder & Simmons
100	-0.28	-0.34	-0.31	-0.18
90	-0.44	-0.45	-0.51	
80	-0.56	-0.50	-0.77	-0.58
70	-0.60	-0.50	-0.59	-0.64
60	-0.54	-0.39	-0.41	-0.54
50	-0.38	-0.24	-0.20	-0.31

The present results compare very favorably with those of Batchelder and Simmons who also used an X-ray technique. The agreement with the data obtained by dilatometric methods of Carr, et al. and Gibbons is only fair.

The Grüneisen parameters (Eq. 1) were calculated by using our thermal expansion data. The values of specific heats[26] and compressibilities were taken from the literature. These results are listed in Table V. The Grüneisen parameters show the same trend as the thermal expansion coefficients and are not of constant value.

2. Diamond

The average lattice parameters of diamond (from three experimental runs) as a function of temperature are shown in Fig. 3 and Table VI. Agreement between our lattice parameters results and

TABLE V

GRÜNEISEN PARAMETERS OF SILICON AT LOW TEMPERATURES

$T^{o}K$	$\alpha x10^{6}/^{o}K$	$V \frac{cm^3}{gm \cdot atom}$	$K_T \frac{Joules}{cm^3}$	$C_p \frac{Joules}{gm \cdot atom\,^{o}K}$	$\gamma = \frac{3\alpha V K_T}{C_p}$
160	0.63	12.05103	$0.98793x10^{5}$	12.7904	0.18
140	0.48	12.05063	$0.98906x10^{5}$	11.0876	0.16
120	0.12	12.05057	$0.98993x10^{5}$	9.2257	0.05
100	-0.28	12.05050	$0.98080x10^{5}$	7.27598	-0.14
90	-0.44	12.05063	$0.99103x10^{5}$	6.28440	-0.25
80	-0.56	12.05083	$0.99133x10^{5}$	5.2760	-0.38
70	-0.60	12.05103	$0.99153x10^{5}$	4.2835	-0.50
60	-0.54	12.05123	$0.99163x10^{5}$	3.2321	-0.60
50	-0.38	12.05137	$0.99163x10^{5}$	2.2058	-0.61

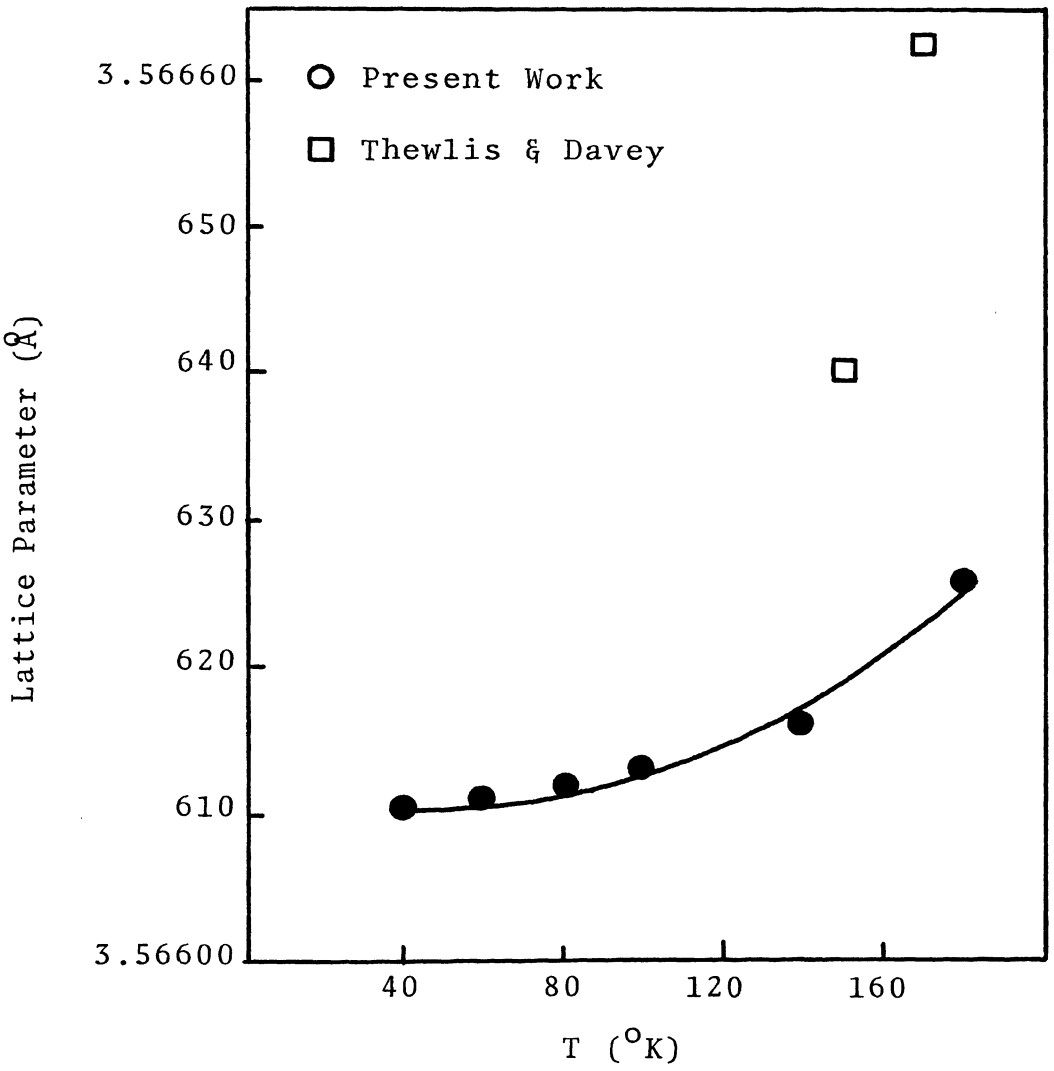

FIGURE 3. Lattice parameters of diamond

TABLE VI

LATTICE PARAMETERS OF DIAMOND AT LOW TEMPERATURES*

$T^{o}K$	Present Results (Å)	Thewlis & Davey (Å)
180	3.56625_5	
170		3.5666
160		
150		3.5664
140	3.56615_9	
100	3.56613	
80	3.56611_9	
60	3.56611_0	
40	3.56610_9	

* No refraction corrections added

those of Thewlis and Davey is very poor. The following equation results for the lattice parameter of diamond as a function of temperature.

$$a(T)\text{Å} = 3.56619 - 4.14 \times 10^{-6}\, T + 7.42 \times 10^{-8}\, T^2 - 5.24 \times 10^{-10}\, T^3 + 1.40 \times 10^{-12}\, T^4 \quad (33)$$

The thermal expansion coefficients were calculated from the above equation and are compared with the published data in Table VII. Once again the agreement is poor in comparison with the results of Thewlis and Davey, but agree quite well with those of Novikova up to 100°K. Below that, the agreement is poor.

The Grüneisen parameters for diamond were not calculated due to the lack of temperature dependence data of compressibility (or bulk-modulus).

D. Discussion:

From the results obtained, it is evident that silicon shows a negative thermal expansion below 120°K. Present thermal expansion data agree very well with those obtained by Batchelder and Simmons who also used an X-ray technique. Results of Carr, et al. and Gibbons do not agree as well. This can be explained in terms of different experimental techniques and samples employed. They employed large single crystals of silicon to study the length changes of the crystal as a function of

TABLE VII

THERMAL EXPANSION COEFFICIENTS OF DIAMOND AT LOW TEMPERATURES

$T^{o}K$	Present Results $\alpha x10^{6}$	Novikova $\alpha x10^{6}$	Thewlis & Davey $\alpha x10^{6}$
160	0.63	0.6	~ 0.4
140	0.32	0.3	
120	0.19	0.2	
100	0.16	0.1	
80	0.15	Slightly Negative	
60	0.09	Slightly Negative	
50	0.01_4	Slightly Negative	

temperature (dilatometric method). In such a setup, it is quite difficult to maintain a set temperature with the use of liquid gases. Secondly, their large single crystal could have had many types of crystal defects, influencing the thermal expansion. Furthermore, their technique of measurement may introduce some errors in the thermal expansion observed. The X-ray diffraction method used here is independent of these problems and factors.

The negative thermal expansion of silicon below 120°K can be explained easily in terms of the Grüneisen parameters and the crystal structure. Since thermal expansion of silicon is clearly related to the Grüneisen parameter, all the discussion pertaining to Grüneisen parameters will also correspond to the thermal expansion behavior. It is shown in Section II that the Grüneisen parameter, γ, is a weighted average of the Grüneisen parameters of various vibrational modes, γ_i (Eq. 12).

$$\gamma = \sum_{i=1}^{3N} \gamma_i C_i / \sum_{i=1}^{3N} C_i \qquad (12)$$

where $\gamma_i = -d \log \omega_i / d \log V$ and C_i are the contributions to specific heat (C_V), from the $i^{\underline{th}}$ mode (Eq. 13).

Now, usually in the crystal, all the γ_i will be positive yielding a positive Grüneisen parameter. That is what is generally expected. As the volume of solid decreases, the frequency of vibration increases giving

rise to a positive γ_i for different vibrational modes. However, if some of the γ_i for some modes are negative and if they start to dominate over the positive γ_i upon cooling, the weighted average γ will be negative and the thermal expansion will also become negative. This concept explains how a negative thermal expansion can be visualized in a crystal. At low temperatures only the transverse acoustic modes are important and some of them must be negative and dominating over the rest of the positive modes to give rise to a negative Grüneisen parameter. To actually prove this hypothesis, a very detailed knowledge of the vibrational spectrum of silicon is needed. From such spectra, the Grüneisen parameters have to be calculated on the first principle basis. Unfortunately, no such details are available at present due to lack of proper experimental (lattice spectrum) data and its clear-cut theoretical treatment.

An intuitive insight can be obtained if one relates the negative thermal expansion of silicon to its crystal structure.[24] The negative thermal expansion is also exhibited by many tetrahedrally bonded covalent substances like InAs, GaAs, InSb, GaSb, α-Sn and vitreous silica, etc., which either possess a diamond cubic or a zincblende type structure. In each of these cases, the atoms have a fourfold coordination, and they are loosely packed structures as compared to a face centered cubic structure (Table VIII).

TABLE VIII

COMPARISON OF DIAMOND CUBIC AND F.C.C. STRUCTURES

Diamond Cubic Structure	Face Centered Cubic Structure
1. For spheres, the diamond cubic structure fills 0.34 of the available space.	1. F.C.C. structure fills 0.74 of the available space.
2. Number of nearest neighbors = 4.	2. N.N.N = 12.

Because of loose packing, the restoring forces for the transverse modes of the bonds may be weak, and these factors may be responsible for negative γ_i's for some transverse modes dominating over the remaining positive ones. The net result is a negative Grüneisen parameter or a negative thermal expansion.

For diamond no such anomalous negative thermal expansion is found down to 40°K despite the theoretical predictions of Dolling and Cowley. But it is quite possible that the magnitude of the negative thermal expansion effect is very small and could not be detected by our experimental techniques. Disagreement with the work of Thewlis and Davey can only be interpreted in terms of poor temperature control and X-ray technique in their experimental setup. By flushing liquid N_2 on the sample, it is very difficult to attain and maintain

a constant temperature. The notion that diamond has an almost constant thermal expansion is evidently false.

V. LATTICE PARAMETERS, THERMAL EXPANSION COEFFICIENTS AND GRÜNEISEN PARAMETERS OF METALS, INTERMETALLIC COMPOUND $A\ell_2Au$ AND LiF IN THE 180^{o}-40^{o}K RANGE

A. Literature Survey:

1. Chromium

No low temperature lattice parameter data are available for chromium. Dilatometric low temperature thermal expansion determinations have been made by Fine, et al.,[31] White[32] and Bolef and Klerk.[15] Fine, et al. used large polycrystalline samples of wrought electrolytic chromium to determine its thermal expansion in the 500^{o}-100^{o}K range. Similar results were obtained by White with polycrystalline samples of chromium of various purities. He found that nitrogen in the chromium samples has a marked effect on the thermal expansion of the latter, also verified by James, et al.[33] No anomalies were found in the thermal expansion of chromium below room temperature by all the mentioned authors.

Chromium becomes antiferromagnetic below 311^{o}K. At this temperature, there is an expected anomaly in the thermal expansion.[31,32,15,33] Bolef and Klerk have also studied the compressibility of chromium below 311^{o}K, finding an anomaly at 120^{o}K. Neutron diffraction studies by Shivane and Takei[34]

indicated a transition between two states of different antiferromagnetic ordering at 121°K.

2. Tungsten

Low temperature lattice parameter data are not listed in the literature. Nix and McMair[36] studied the thermal expansion of a polycrystalline tungsten sample down to 120°K with a dilatometric technique. Corruccini and Gniewek[37] used the Grüneisen relation to extrapolate the thermal expansion data of Nix and McNair below 120°K. In their work on the bulk modulus, Featherston and Neighbors[38] found that b.c.c 4d-5d metals like Ta, W and Mo behave anomalously, the anomalous range of tungsten being 200°-140°K. For an explanation, they propose antiferromagnetic ordering in this temperature range and stipulate further that thermal expansion of tungsten should be anomalous in the same temperature range.

3. Copper

Simmons and Balluffi[40] studied the thermal expansion of single crystals of copper (99.996%) from 100°-8°K by an X-ray method. Unfortunately, they do not report their lattice parameters but only the calculated thermal expansion coefficients. All of the other data on the thermal expansion of copper were obtained with dilatometric methods.

Buffington and Latimer[41] investigated the thermal expansion of copper from 300°-120°K by a Fizeau interferrometer using a polycrystalline copper sample of unknown purity, employing a quartz standard. Nix and McNair[42] studied the thermal expansion of polycrystalline copper (99.979%) using a dilatometric-interferrometric technique in the temperature range of 300°-100°K. Bijl and Pullan[43] measured the thermal expansion of polycrystalline samples (99.98%) using a capacitance-dilatometer. Rubin, et al.[44] investigated the thermal expansion of single crystals of copper from 300°-40°K with a Fizeau interferrometer.

4. Nickel and iron

No low temperature lattice parameter data for nickel and iron are available at present. Nix and McNair[42] determined the thermal expansion coefficients of polycrystalline samples of nickel (99.9%) and iron (99.992%) by a dilatometric method in the range of 300°-120°K. Corruccini and Gniewek[37] have used the Grüneisen relation to extrapolate these data below 120°K. Fraser and Hallett[45] made the thermal expansion study of polycrystalline samples of nickel and iron (of unknown purities) by a dilatometric technique.

5. $A\ell_2Au$

Low temperature lattice parameters of this compound cannot be found in the literature. Some studies of phase extent, lattice parameters and expansion coefficients of the compound were made at room temperature by Straumanis and Chopra.[48] $A\ell_2Au$ has a cubic CaF_2-type structure, and it contains 78.4954% (b.w.) of gold.

6. LiF

Himmler, et al.[53] studied the lattice expansivity ($\Delta a/a$) of LiF of unknown purity using a liquid He cryostat for high precision measurements between 350° and 4°K with a diffractometer. They report the expansivity $\Delta a/a_{ref}=(a_T-a_{ref})/a_{ref}$, where a_T is the lattice parameter at some temperature and a_{ref} that at 4.2°K (a_{ref}=4.005141 Å). Yates and Panter[54] studied the thermal expansion and Grüneisen parameters of single crystals of LiF by a dilatometric method. The single crystals had an impurity range of 10-100 ppm.

B. Experimental Details:

Powder samples of Cr, W, Cu, Ni and Fe of 8-10μ average particle size were obtained from Koch Light Labs, Inc., Colnbrook, England. These gave sharp and uniform diffraction lines when proper radiation was used, so no further heat treatments were performed. An additional

Fe sample of higher purity (99.999%) was also studied to observe the effects of impurities on the thermal expansion of Fe at low temperatures. Finely divided powder of $A\ell_2Au$ was available.[48] A fine powder of LiF was prepared by grinding the coarse powder and then sieving it through a special 10μ sieve.

Lattice parameters were calculated by measuring the distance bewteen the appropriate high angle diffraction lines. The X-ray wavelength and high angle reflection used for each material is listed below.

Sample	Wavelength λ(Å)		Diffraction Plane
Cr(99.3%)	Co $K_{\alpha_{(1)}}$	λ=1.78892	(310) α_1
W(99.9%)	Co $K_{\alpha_{(1)}}$	λ=1.78892	(222) α_1
Cu(99.7%)	Co $K_{\alpha_{(1)}}$	λ=1.78892	(400) α_1
Ni(99.9%)	Cu $K_{\alpha_{(1)}}$	λ=1.54051	(420) α_1
Fe(99.9%+99.999%)	Co $K_{\alpha_{(1)}}$	λ=1.78892	(310) α_1
$A\ell_2Au$	Cu $K_{\alpha_{(1)}}$	λ=1.54051	(553) α_1
LiF	Cr $K_{\alpha_{(1)}}$	λ=2.28962	(222) α_1

Usually three exposures at each of the temperatures of 40°, 60°, 80°, 100°, 140° and 180°K were taken. For Cr additional runs in the vicinity of 120°K were made to check the anomaly found by Bolef and Klerk.

C. Results:

1. Chromium

Lattice parameters of Cr as a function of temperature for the 180^{o}-40^{o}K range are expressed by the equation:

$$a\,\mathring{A}(T) = 2.88257 - 5.90\times10^{-6}T + 5.98\times10^{-8}T^{2} \qquad (34)$$

The average lattice parameters of three runs (18 individual experimental points) are shown in Table IX and Fig. 4. Lattice parameter studies in the vicinity of 120^{o}K did not reveal any anomalous behavior. Thermal expansion coefficients were calculated from Eq. (34) and Grüneisen parameters (Eq. 1) were determined by using these thermal expansion coefficients and the literature values of specific heat[35] and compressibility.[15] The data obtained are compared with those of Fine, et al. and White in Fig. 5. As can be seen, the results are in good agreement with the published data. The Grüneisen parameters are listed in Table IX together with the lattice parameters and thermal expansion coefficients, etc. Table IX shows that the Grüneisen parameters of chromium decrease with temperature.

2. Tungsten

The average lattice parameters of tungsten

TABLE IX

LATTICE PARAMETERS, THERMAL EXPANSION COEFFICIENTS, ETC., AND GRÜNEISEN PARAMETERS OF CHROMIUM AT LOW TEMPERATURES

Temp ^{o}K	Lattice* Parameter Å	$\alpha/^{o}K$	C_p $J/g\cdot atom\,^{o}K$	χ $cm^3/Joules$	V $cm^3/gm\cdot atom$	$\gamma=\frac{3\alpha\cdot V}{C_p\,\chi}$
180	2.88345	5.41×10^{-6}	18.770	5.45×10^{-6}	7.2200	1.15
140	2.88290	3.75×10^{-6}	15.391	5.35×10^{-6}	7.2160	0.99
100	2.88257	2.10×10^{-6}	10.035	5.30×10^{-6}	7.2140	0.85
80	2.88250	1.27×10^{-6}	6.604	5.26×10^{-6}	7.2130	0.78
60	2.88245	0.44×10^{-6}	3.229	5.30×10^{-6}	7.2120	0.57
40	2.88240					

* Not corrected for refraction

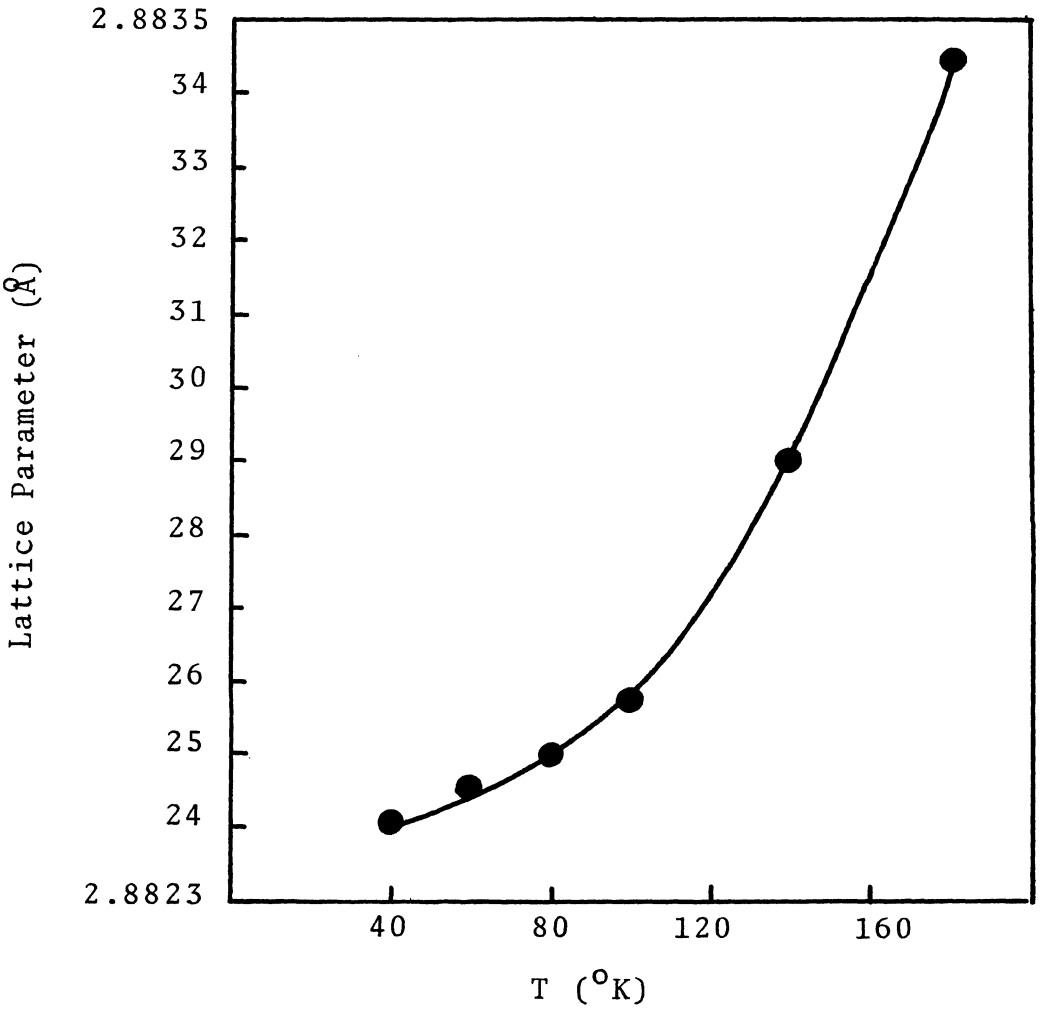

FIGURE 4. Lattice parameters of chromium

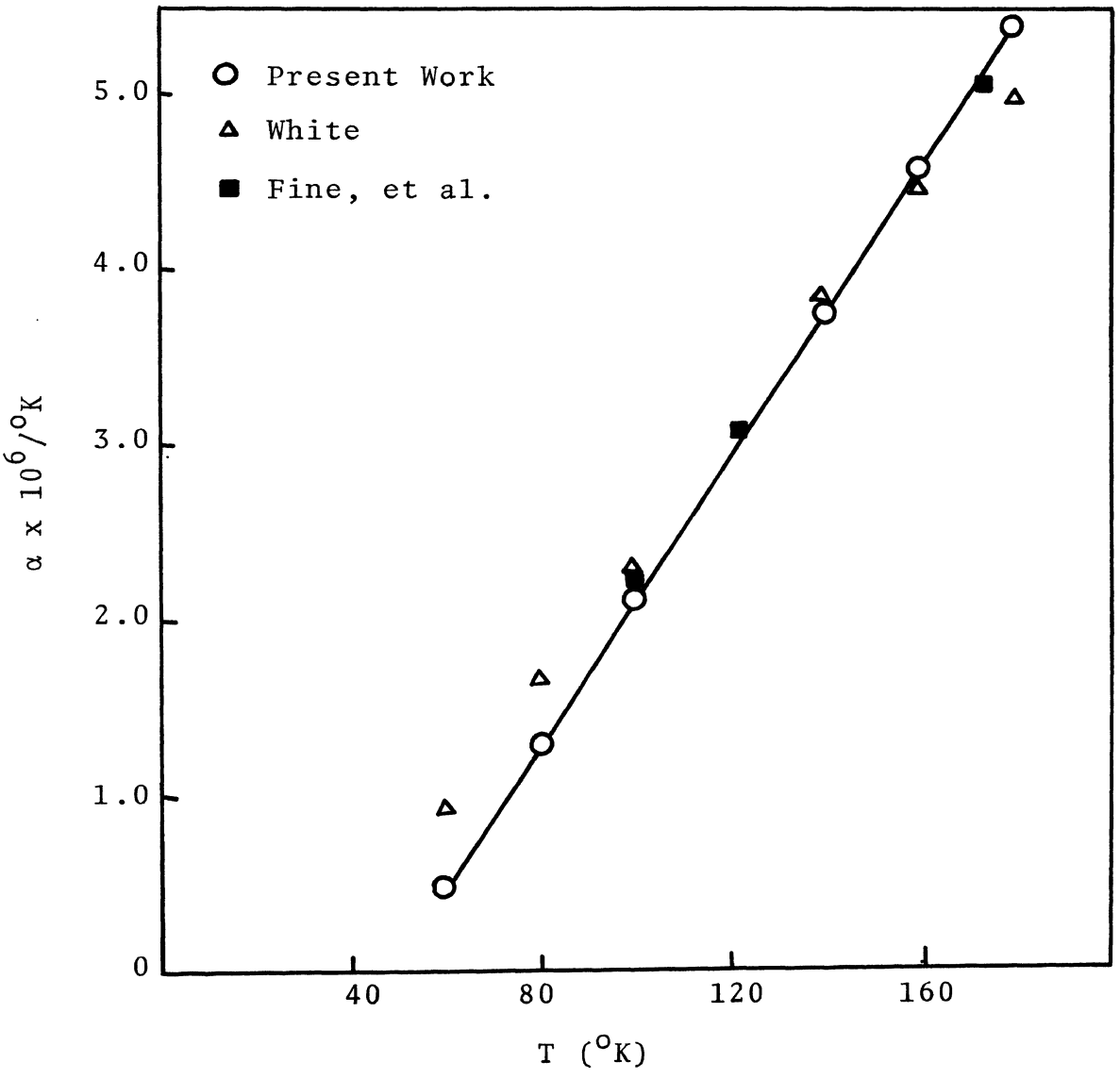

FIGURE 5. Thermal expansion of chromium

(obtained from three separate runs) are shown in Fig. 6 and tabulated in Table X together with the thermal expansion coefficients and Gruneisen parameters. The following equation relates the lattice parameter of tungsten in the 180^{o}-40^{o}K range as a function of temperature:

$$a\,\text{Å}(T)=3.16277-3.81\times10^{-6}T+7.08\times10^{-8}T^{2}-1.02\times10^{-10}T^{3} \quad (35)$$

Thermal expansion data obtained from the above equation are compared with those of Nix and McNair in Fig. 7. Since their data terminate at 120^{o}K, the present results are compared with the extrapolated values of Corruccini and Gneiwek. The agreement is poor.

In the Grüneisen parameter calculations, our thermal expansion coefficients and published data for specific heats[35] and bulk modulus[39] were used (Table X).

3. Copper

The average lattice parameters of copper obtained in this investigation from three separate runs are plotted in Fig. 8 and tabulated in Table XI (along with the thermal expansion coefficients and Grüneisen parameters). The following equation relates the lattice parameters as a

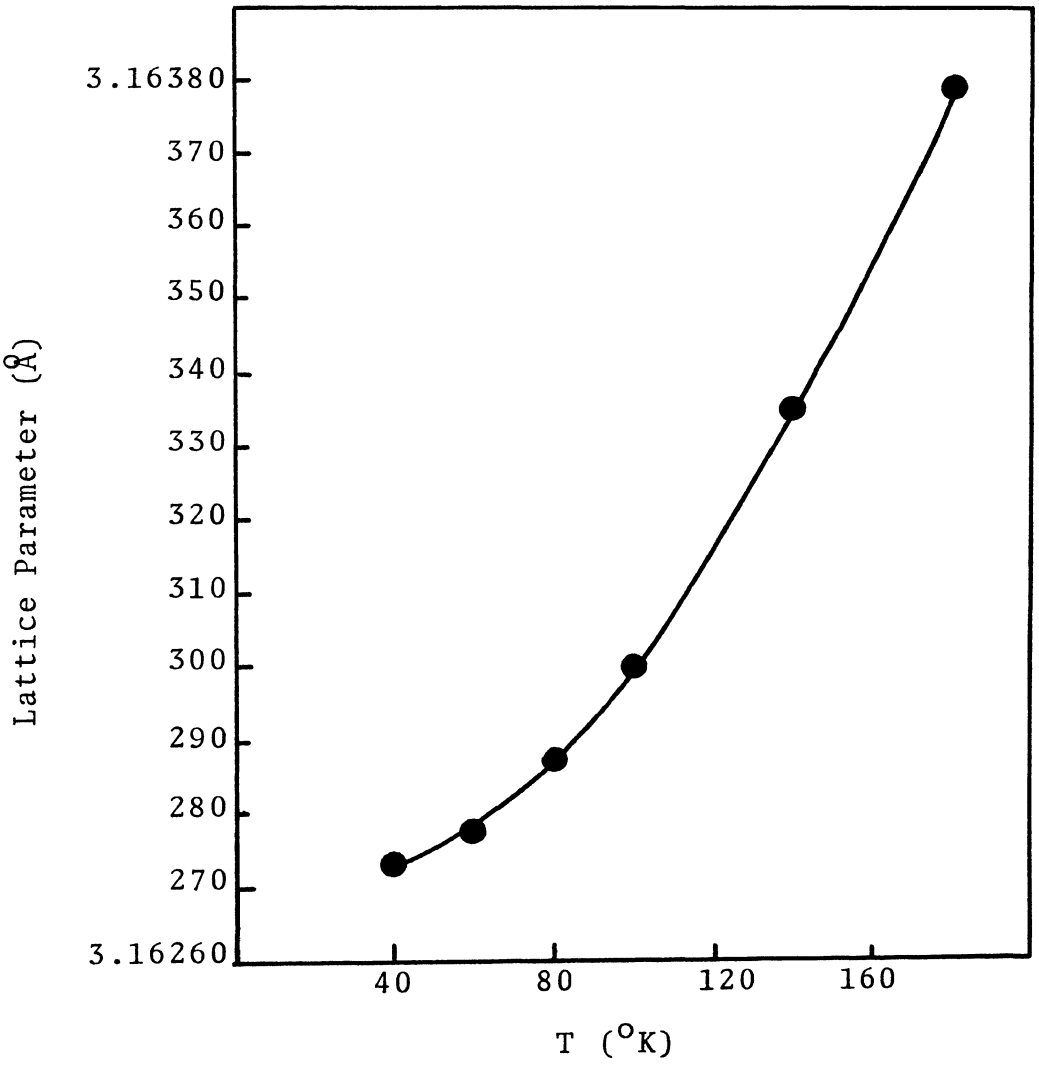

FIGURE 6. Lattice parameters of tungsten

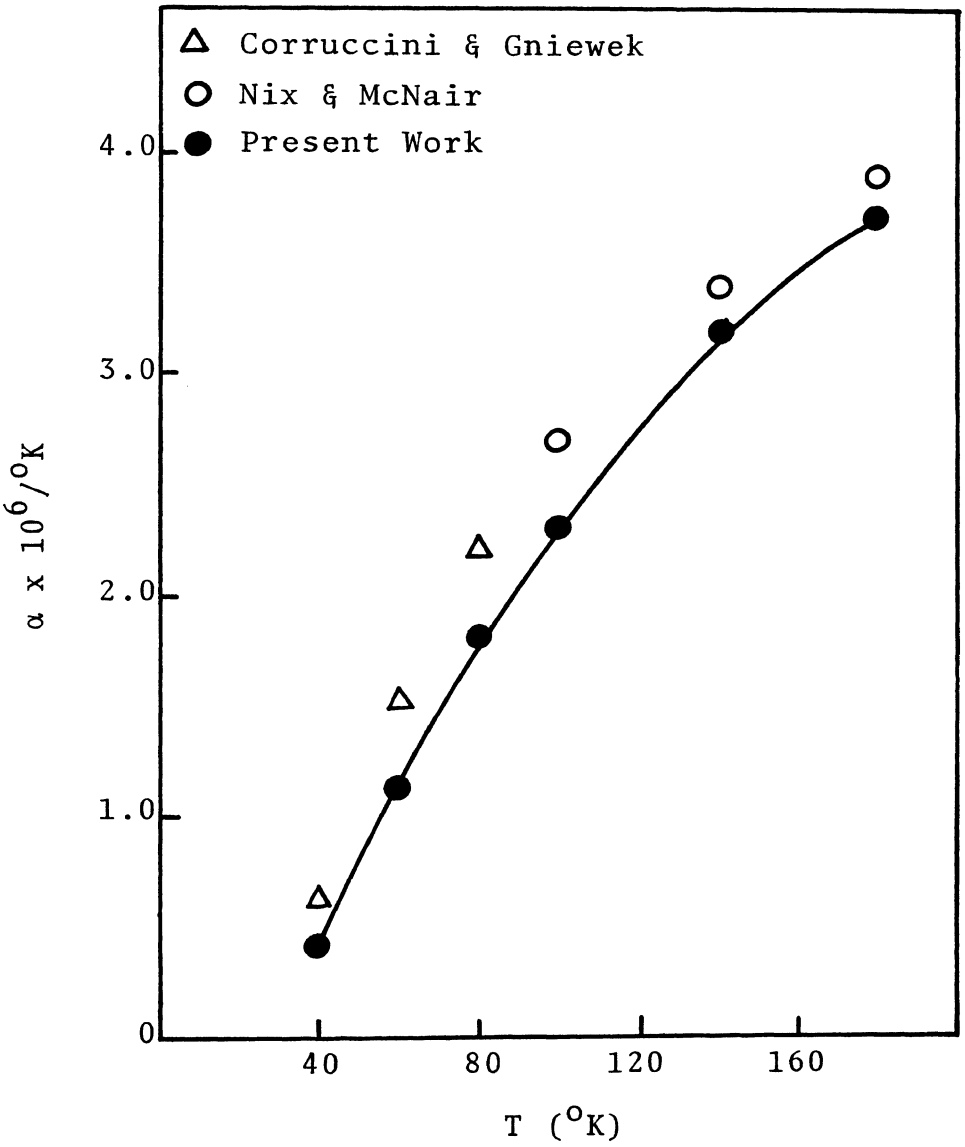

FIGURE 7. Thermal expansion of tungsten

TABLE X

LATTICE PARAMETERS, THERMAL EXPANSION COEFFICIENTS, ETC. AND GRÜNEISEN PARAMETERS OF TUNGSTEN AT LOW TEMPERATURES

$T^{\circ}K$	a* Å	$\alpha/^{\circ}K$	C_p Joules/gm·atom$^{\circ}K$	K_T Joules/cm^3	V cm^3/gm·atom	γ
180	3.16379	3.7×10^{-6}	22.4297	3.1017×10^{5}	31.6682	1.47
140	3.16335	3.2×10^{-6}	20.2235	3.1110×10^{5}	31.6550	1.39
100	3.16300	2.3×10^{-6}	16.3259	3.1210×10^{5}	31.6445	1.26
80	3.16287	1.8×10^{-6}	13.1453	3.1278×10^{5}	31.6406	1.20
60	3.16277	1.1×10^{-6}	8.8800	3.1345×10^{5}	31.6375	1.14
40	3.16273	0.4×10^{-6}	3.3828	3.1450×10^{5}	31.6363	1.14

* Not corrected for refraction

a function of temperature in the 180°-40°K range:

$$a\ \text{Å}(T) = 3.602472 + 6.99\times10^{-6}T + 1.45\times10^{-7}T^2 \qquad (36)$$

The thermal expansion coefficients were calculated from the above equation and are compared with the published data in Table XII. These are also plotted in Fig. 9. The agreement is very good. The Grüneisen parameters were calculated in the usual manner, taking our α values and literature values for specific heats[35] and bulk modulus.[45] Results of these calculations are shown in Table XI.

4. Nickel

The following equation expresses the lattice parameters of nickel as a function of temperature in the 180°-40°K range:

$$a\ \text{Å}(T)=3.516028-8.938\times10^{-6}+1.767\times10^{-7}T^2-1.7106\times10^{-10}T^3 \qquad (37)$$

Thermal expansion coefficients were calculated from the above equation. Grüneisen parameters were calculated from our values of α and literature data for C_p[35] and K_T.[46] Lattice parameter results are shown in Fig. 10 and Table XIII. The thermal expansion results are compared with the published data in Fig. 11. The agreement is very good. Thermal expansion coefficients are also tabulated together with the lattice and Grüneisen parameters

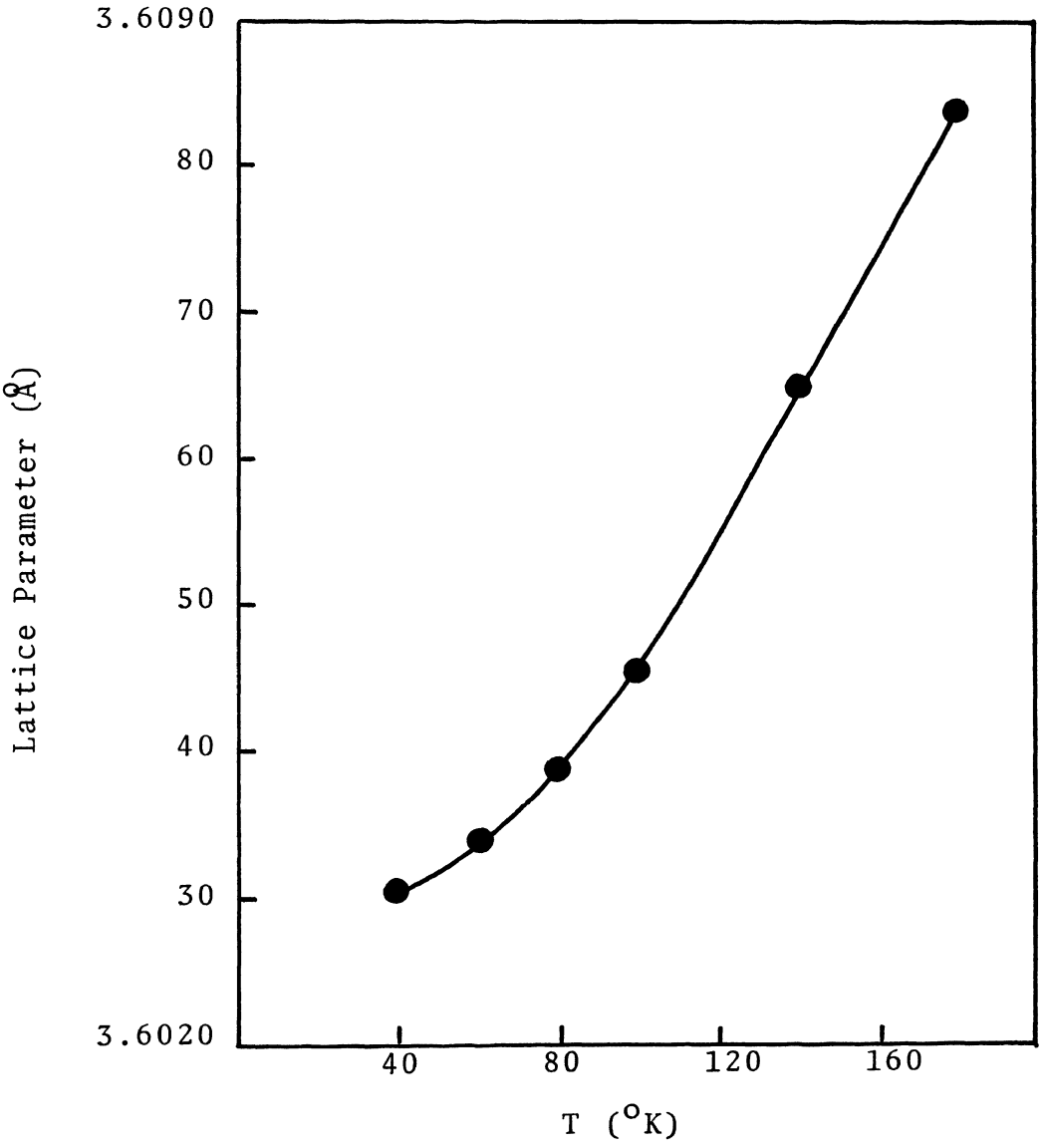

FIGURE 8. Lattice parameters of copper

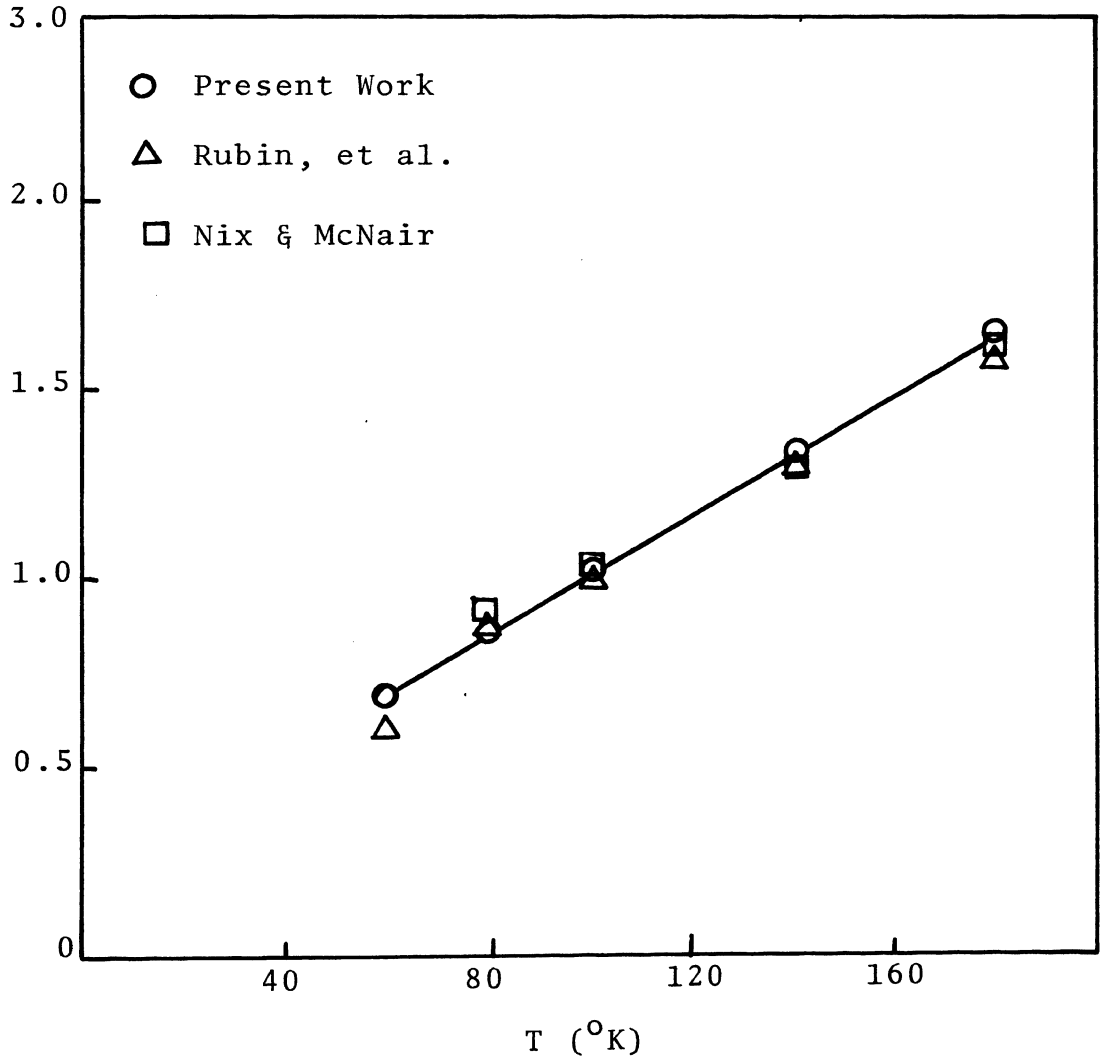

FIGURE 9. Thermal expansion of copper

TABLE XI

LATTICE PARAMETERS, THERMAL EXPANSION COEFFICIENTS, ETC. AND GRÜNEISEN PARAMETERS OF COPPER AT LOW TEMPERATURES

$T^{o}K$	Lattice* Parameter Å	$\alpha/^{o}K^{-1}$	C_p Joules/gm·atom^{o}K	K_T Joules/cm^3	V cm^3/g·atom	$\gamma=\frac{3\alpha VK_T}{C_p}$
180	3.60836	1.64×10^{-5}	21.894	13.759×10^{4}	7.075	2.2
140	3.60648	1.32×10^{-5}	19.888	13.899×10^{4}	7.063	2.0
100	3.60455	1.00×10^{-5}	15.885	14.031×10^{4}	7.052	1.9
80	3.60386	0.81×10^{-5}	13.026	14.092×10^{4}	7.048	1.9
60	3.60340	0.66×10^{-5}	8.705	14.146×10^{4}	7.045	2.3
40	3.60306					

* Not corrected for refraction

TABLE XII

THERMAL EXPANSION COEFFICIENTS OF COPPER

	$\alpha x 10^5$					
Temp ^{o}K	Present Work	Buffington & Latimer	Nix & McNair	Bijl & Pullan	Rubin et al.	Simmons & Bulluffi
180	1.64	1.5	1.5		1.5	
160		1.4		1.40	1.4	
140	1.32	1.3	1.35	1.30	1.32	
120		1.2			1.20	
100	1.00		1.00	1.07	1.05	
80	0.81			0.88	0.83	0.85
60	0.66			0.46	0.55	0.56

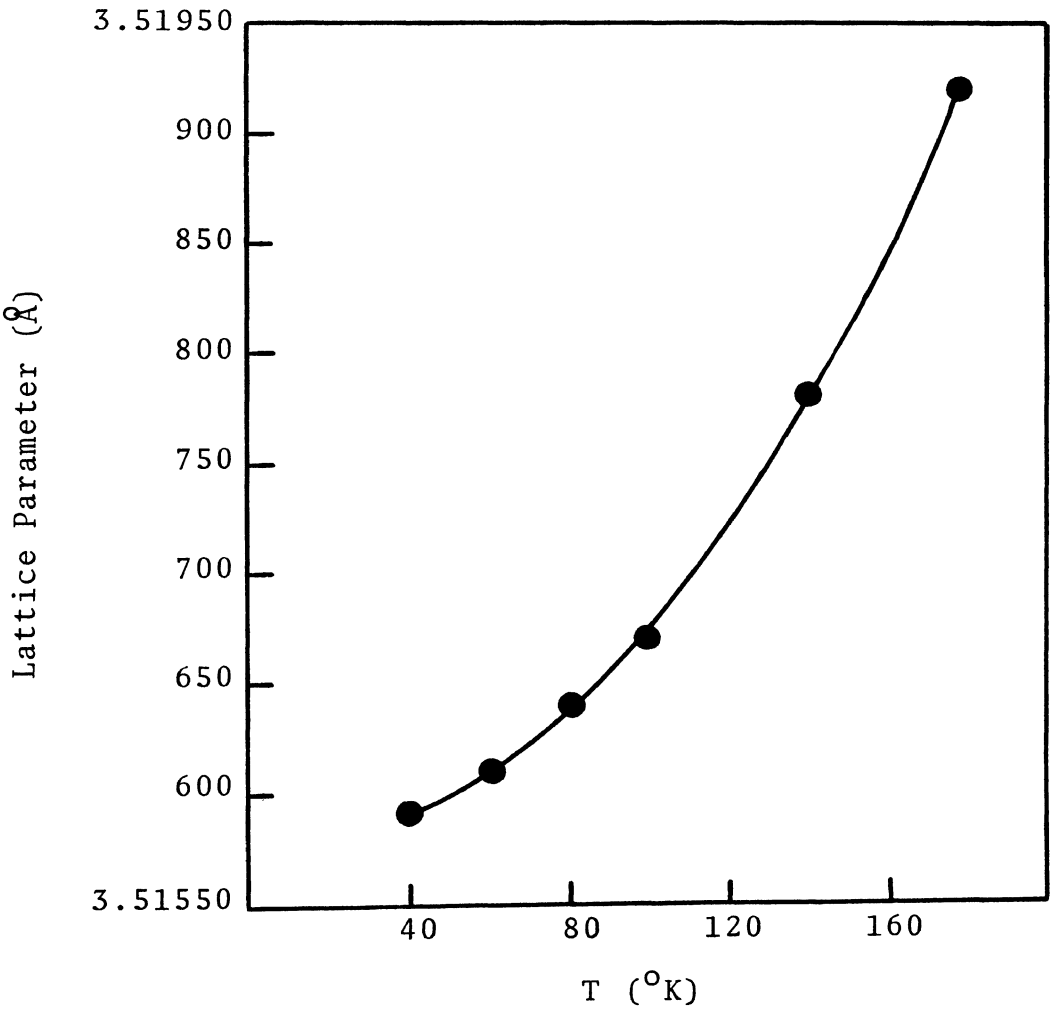

FIGURE 10. Lattice parameters of nickel

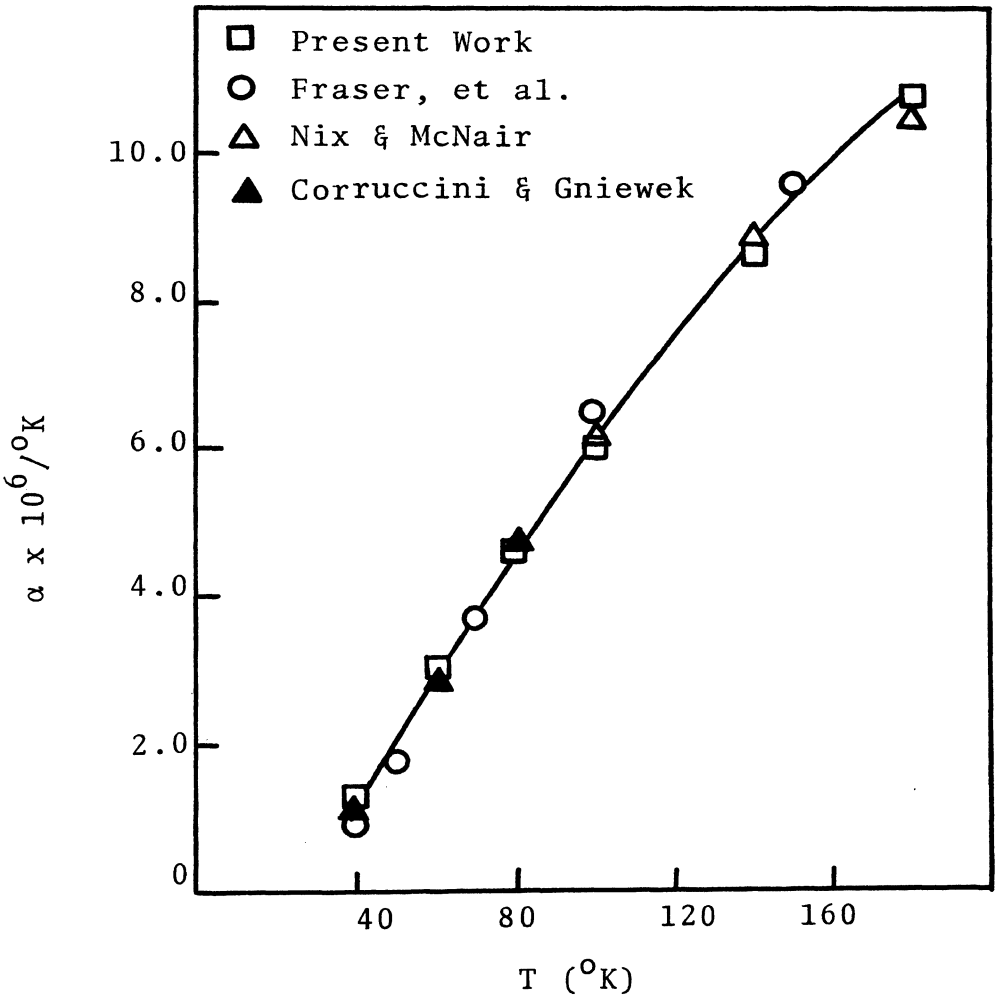

FIGURE 11. Thermal expansion of nickel

TABLE XIII

LATTICE PARAMETERS, THERMAL EXPANSION COEFFICIENTS AND GRÜNEISEN PARAMETER OF NICKEL

$T^{o}K$	a* Å	$\alpha x10^{6}/^{o}K$	V cm^{3}/mole	C_p Joules/mole^{o}K	K_T Joules$x10^{5}/cm^{3}$	$\gamma=\frac{3\alpha VB}{C_p}$
180	3.51915	10.8	6.57008	21.429	1.855	1.84
140	3.51777	8.67	6.56235	18.435	1.862	1.72
100	3.51672	6.05	6.55648	13.621	1.870	1.63
80	3.51637	4.57	6.55452	10.157	1.872	1.65
60	3.51608	2.96	6.55290	6.047	1.873	1.80
40	3.51594	1.25	6.55212	2.237	1.875	2.06

* Not corrected for refraction

in Table XIII. The thermal expansion of nickel shows a normal behavior for a metal. Grüneisen parameters increase slightly at lower temperatures.

5. Iron

The average lattice parameters of 99.9% Fe (18 experimental points) and 99.999% Fe (12 experimental points) are shown in Fig. 12 and in Table XIV. One observes a distinct tendency for the lattice parameters of higher purity iron to be lower and the difference, Δa, between the two Fe samples decreases with temperature. However, it would be premature to speculate as to the effects of impurities on the thermal variation of the lattice parameters of Fe, since the standard deviation for the parameters is, $\sigma=\pm 3.8\times10^{-5}$.

$$a\,\mathring{A}(T)=2.86690-5.4106\times10^{-6}T+9.545\times10^{-8}T^2 \qquad (38)$$

Above, Eq. (38) relates the lattice parameters of Fe (99.9%) as a function of temperature in the 180^{o}-40^{o}K range. Thermal expansion coefficients were calculated for this equation, and the results are compared with the published data in Fig. 13 and Table XV together with the Grüneisen parameters. The agreement is quite good. Grüneisen parameters of Fe were calculated from our α data and literature data for C_p[35] and K_T[47] which are shown in Table XV.

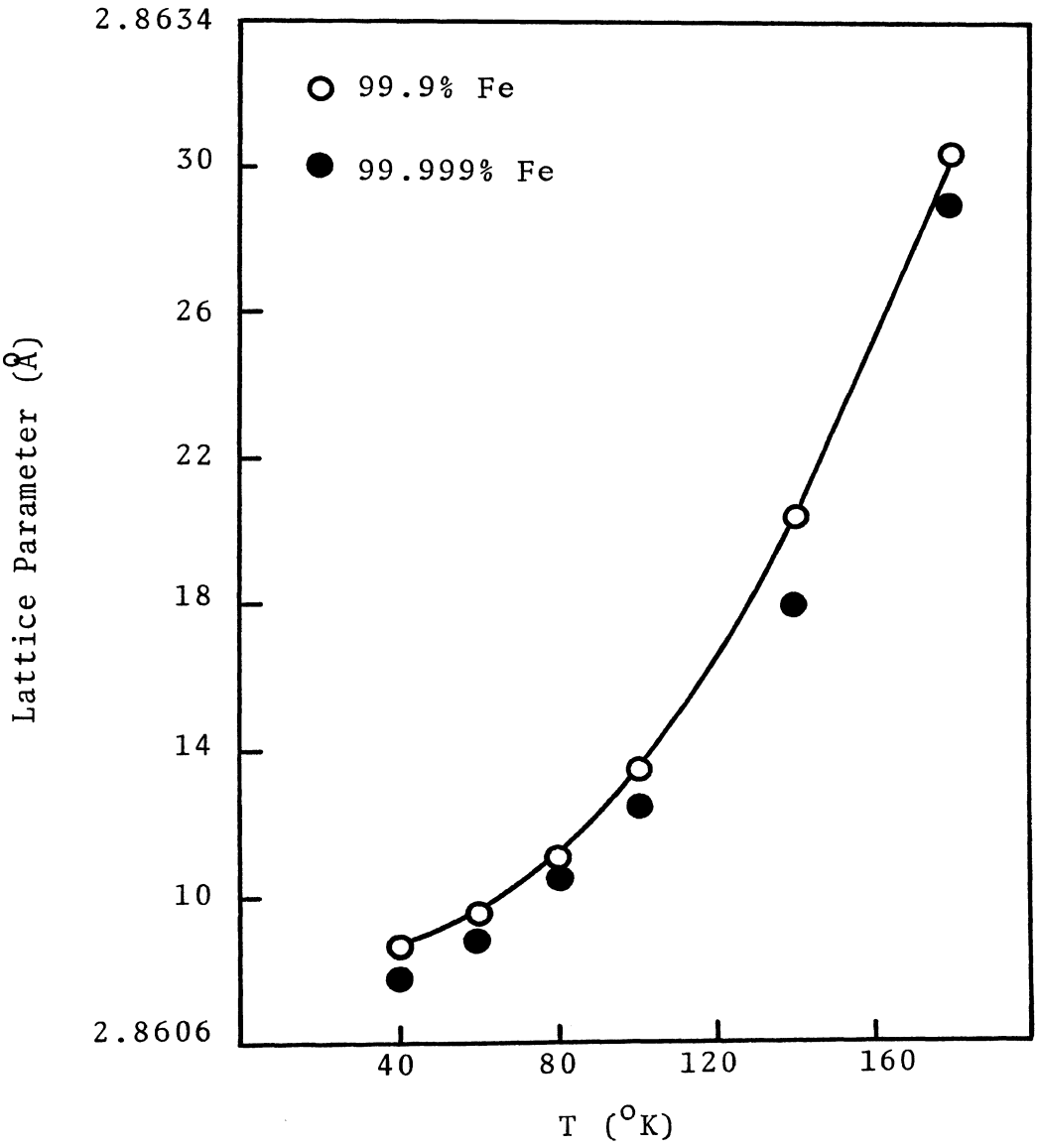

FIGURE 12. Lattice parameter of iron

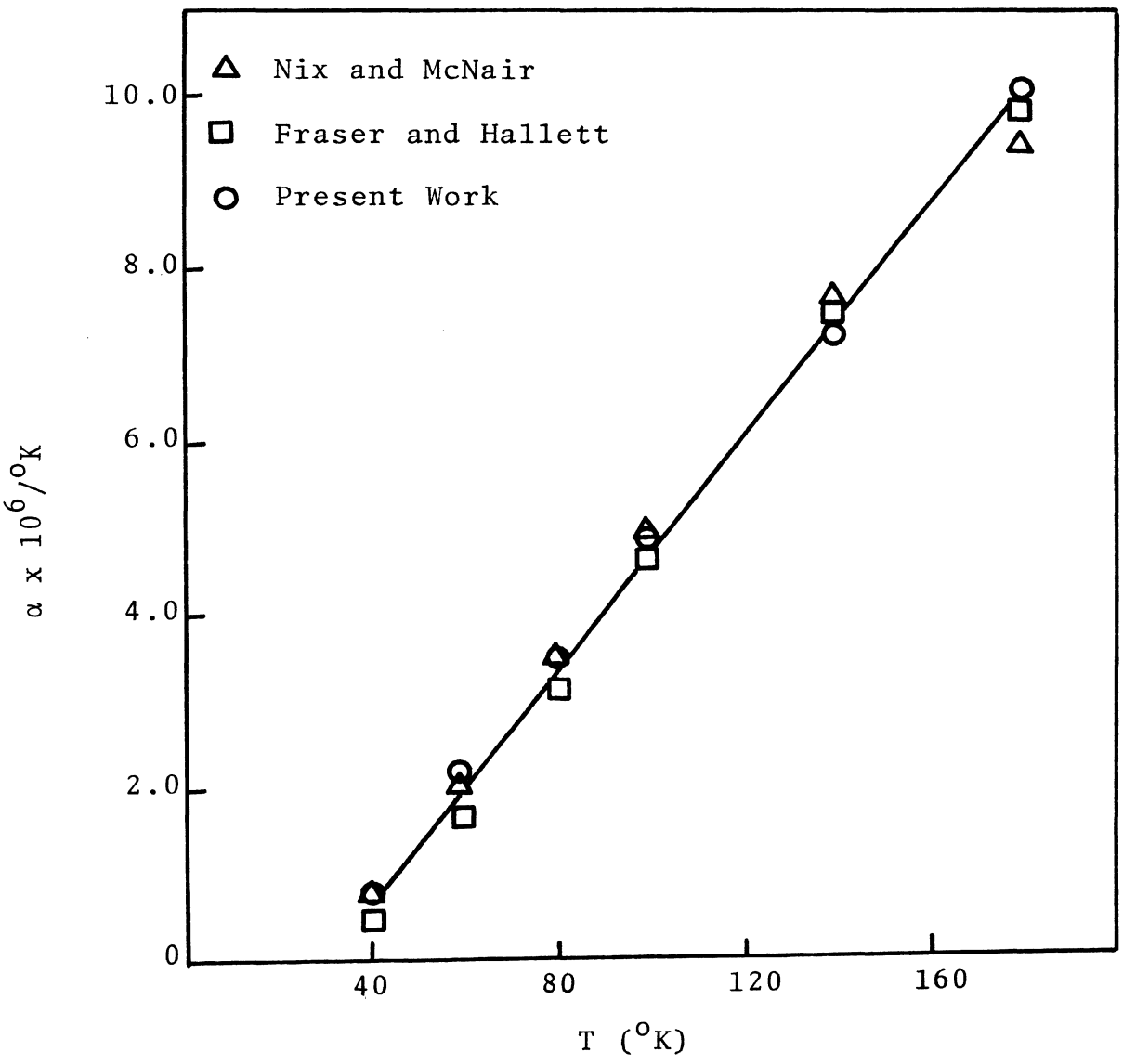

FIGURE 13. Thermal expansion of iron

TABLE XIV

LATTICE PARAMETERS* OF 99.9% AND 99.999% Fe

$T^{o}K$	99.9% a(Å)	99.999% a(Å)	Δa (Å)
180	2.86304	2.86289	.00015
140	2.86204	2.86178	.00026
100	2.86134	2.86125	.00009
80	2.86110	2.86106	.00004
60	2.86095	2.86090	.00005
40	2.86086	2.86077	.00009

* Refraction corrections not included

TABLE XV

THERMAL EXPANSION COEFFICIENTS AND GRÜNEISEN PARAMETER OF IRON

$T^{o}K$	$\alpha x10^{6}/^{o}K$	V $cm^{3}/g\cdot atom$	K_T $Joules x10^{5}/cm^{3}$	C_p $Joules/g\cdot atom^{o}K$	$\gamma=\frac{3\alpha VK_T}{C_p}$
180	10.11	7.06822	1.699	20.17	1.70
140	7.44	7.06298	1.707	17.32	1.71
100	4.78	7.05533	1.716	12.00	1.72
80	3.45	7.05356	1.721	8.62	1.72
60	2.11	7.05245	1.727	4.81	1.72
40	0.79	7.05178	1.729	1.57	1.72

6. $A\ell_2Au$

The following equation relates the lattice parameters of $A\ell_2Au$ to the temperature in the 180^{o}-$40^{o}K$ range:

$$a\,\mathring{A}(T)=5.9863-3.236\times10^{-6}T+1.632\times10^{-7}T^{2} \qquad (39)$$

The average lattice parameters are plotted in Fig. 14 and tabulated in Table XVI. The thermal variation of the lattice parameters of $A\ell_2Au$ is normal. The thermal expansion coefficients of the compound are shown in Fig. 15 and Table XVI. The Grüneisen parameters of $A\ell_2Au$ cannot be calculated due to the lack of C_V and K_T data.

7. LiF

The following equation was derived for the lattice parameters of LiF as a function of temperature in the 180^{o}-$40^{o}K$ range:

$$a\,\mathring{A}(T)=4.005971-3.113\times10^{-5}T+3.66\times10^{-7}T^{2} \qquad (40)$$

The average lattice parameters (from three separate runs) are shown in Fig. 16 and Table XVII. The lattice expansivity $\Delta a/a_{ref}$ (a_{ref}=4.005141 Å at $4.2^{o}K$ from Himmler, et al.) for LiF is compared with the published data in Table XVII. As evident from Table XVII, our $\Delta a/a$ results are in excellent agreement with those of Himmler, et al. The

TABLE XVI

LATTICE PARAMETERS AND THERMAL EXPANSION COEFFICIENTS OF $A\ell_2Au$

T^oK	a (Å)*	$\alpha x10^6/^oK$
180	5.99101	9.3
140	5.98905	7.1
100	5.98761	4.9
80	5.98709	3.8
60	5.98669	2.7
40	5.98643	1.6

TABLE XVII

LATTICE PARAMETERS AND LATTICE EXPANSIVITY $\Delta a/a_{ref}$ FOR LiF

T^oK	a* Å	Present Work $\Delta a/a_{ref}$† $x10^3$	Himmler, et al. $\Delta a/a_{ref} x10^3$
180	4.01190	1.688	1.687
140	4.00838	0.809	0.808
100	4.00635	0.302	0.304
80	4.00570	0.140	0.139
60	4.00535	0.052	0.052
40	4.00517	0.008	0.007

* Not corrected for refraction

† a_{ref}=4.005141 Å

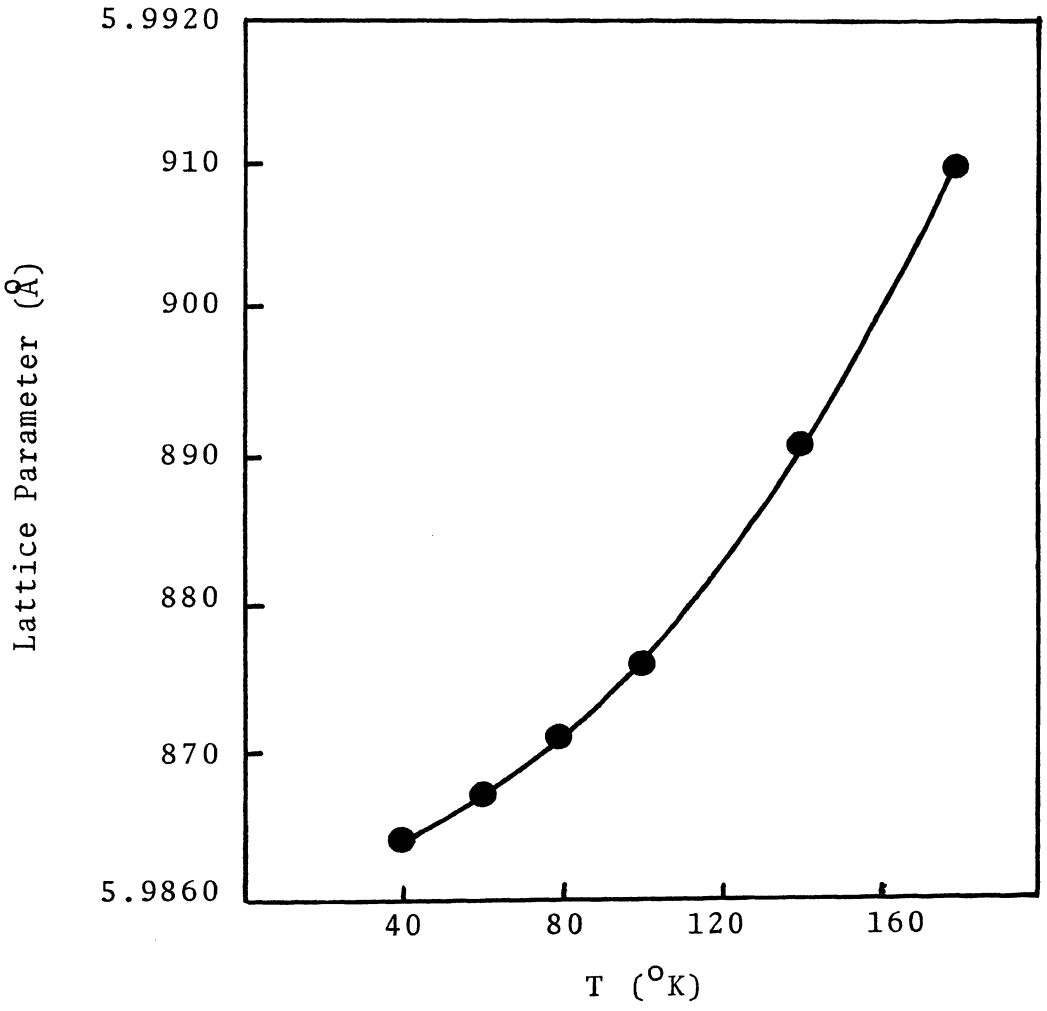

FIGURE 14. Lattice parameters of Al_2Au

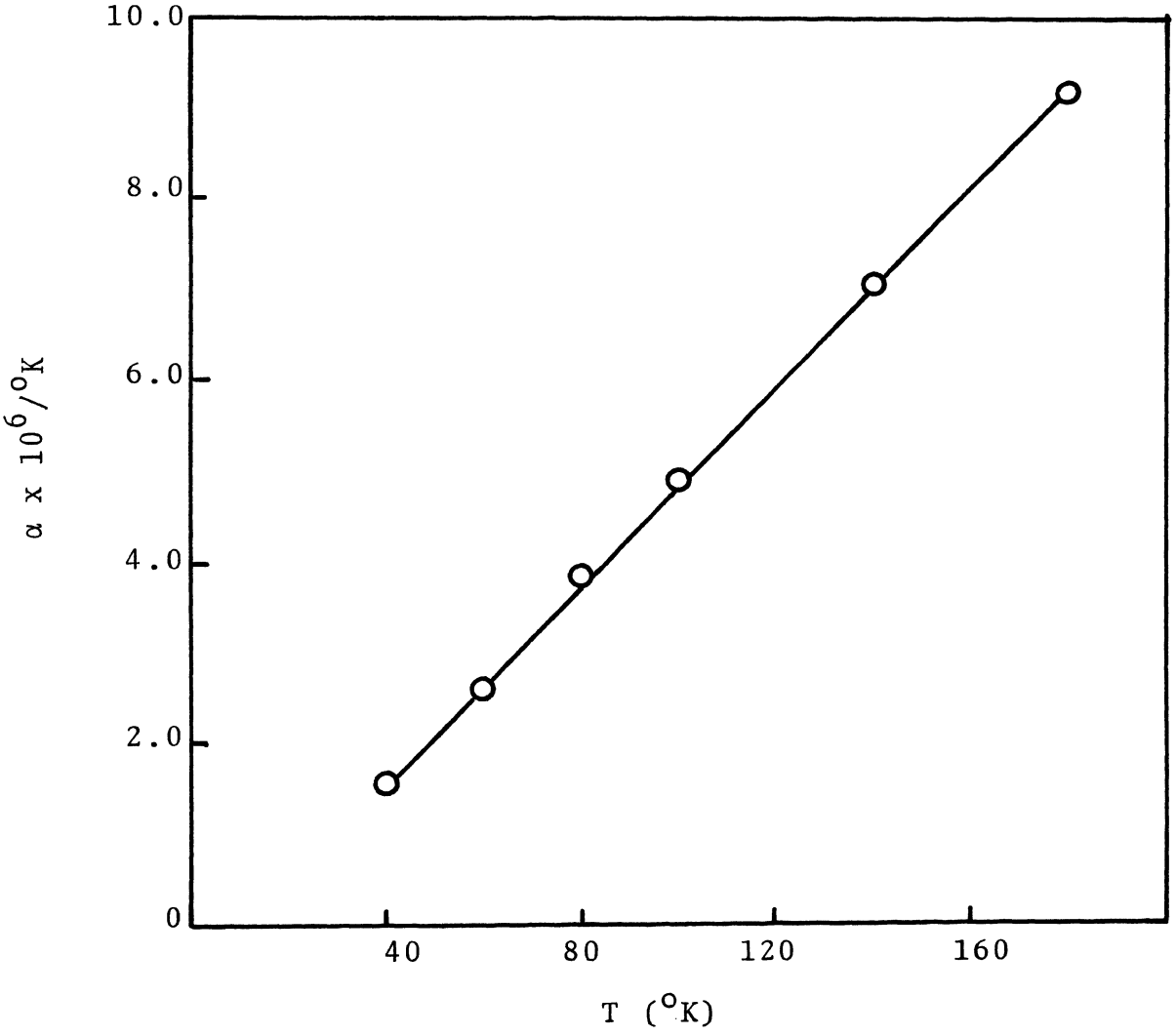

FIGURE 15. Thermal expansion of $A\ell_2Au$

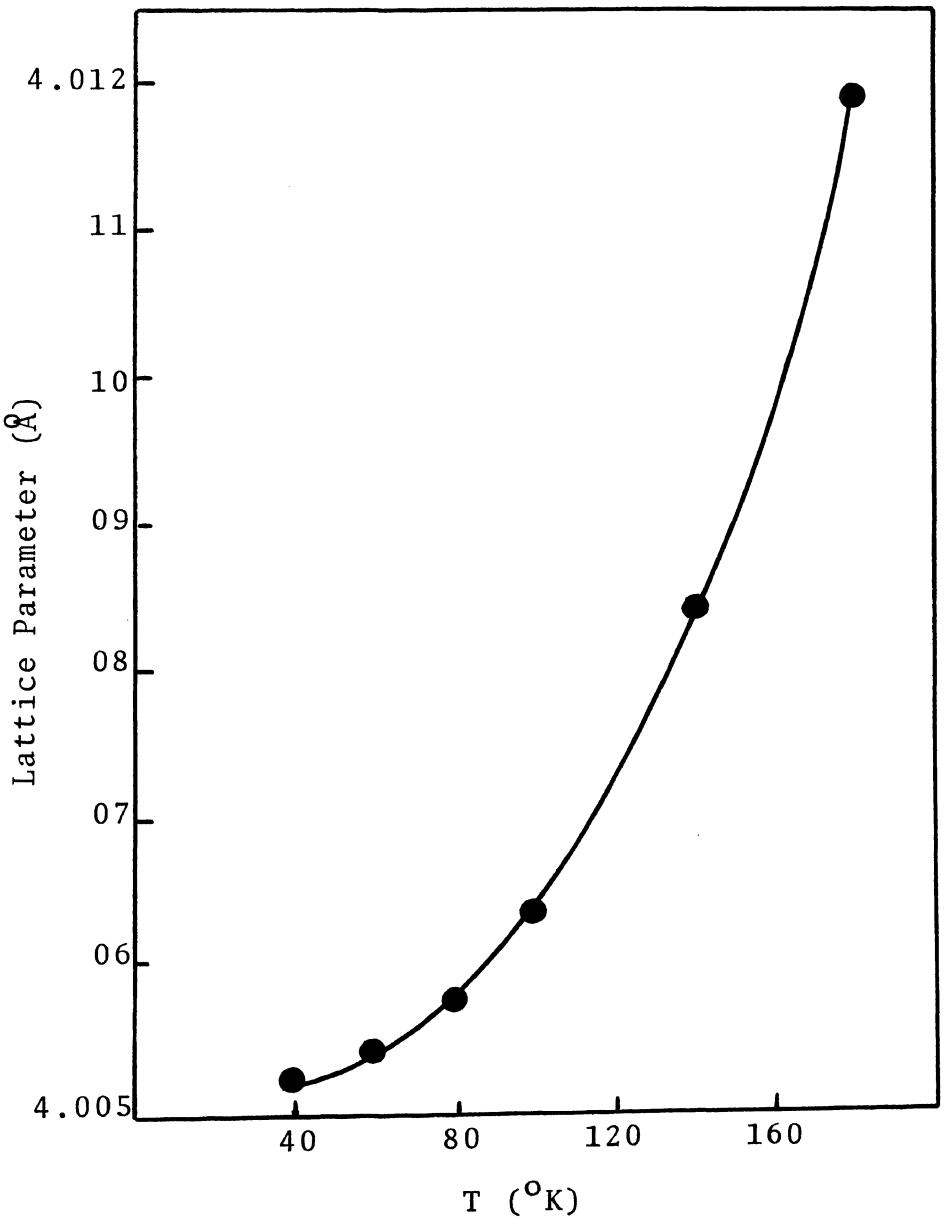

FIGURE 16. Lattice parameters of LiF

thermal expansion coefficients were calculated from Eq. (40) and are compared with those of Yates and Panter in Table XVIII and Fig. 17. The agreement in this case is also very good. The Grüneisen parameters were calculated using the literature values of C_p[55] and χ_T[56] and they have a constant value in the 180^{o}-40^{o}K range.

D. Discussion:

When comparing the results obtained in this investigation with those of previous researchers, one must keep in mind the differences in the methods and in samples used. The X-ray method used in this investigation is an absolute method to study the lattice expansion and it has the following advantages over other methods which use various size bulk samples (polycrystalline or single crystal) and liquid gases:

i) It determines the size of the crystal unit cell directly. From this point of view, the results obtained by other methods using bulk specimens for the study of the macroscopic and microscopic length changes might be affected by the grain boundaries, voids, microcracks and other structural defects.

ii) It is an absolute method; most other methods must, by their nature, use a reference standard at the temperature of the specimen.

TABLE XVIII

THERMAL EXPANSION COEFFICIENTS AND GRÜNEISEN PARAMETERS OF LiF

	$\alpha x10^6$					$\gamma=\frac{3\alpha V}{C_V \chi_T}$	
T^oK	Present Work	Yates & Panter	$V\frac{cm^3}{g\cdot mole}$	$C_p\frac{Joules}{pmole^oK}$	$\chi_T\frac{cm^3}{Joules}x10^5$	Present Work	Yates & Panter
180	24.53	23.8	9.72226	29.43	1.48	1.64	1.61
140	17.27	17.3	9.69669	21.41	1.46	1.61	1.59
100	9.98	9.7	9.68196	12.88	1.44	1.56	1.57
80	6.33	6.0	9.67725	7.93	1.44	1.61	1.61
60	2.68	2.6	9.67472	3.43	1.43	1.60	1.60

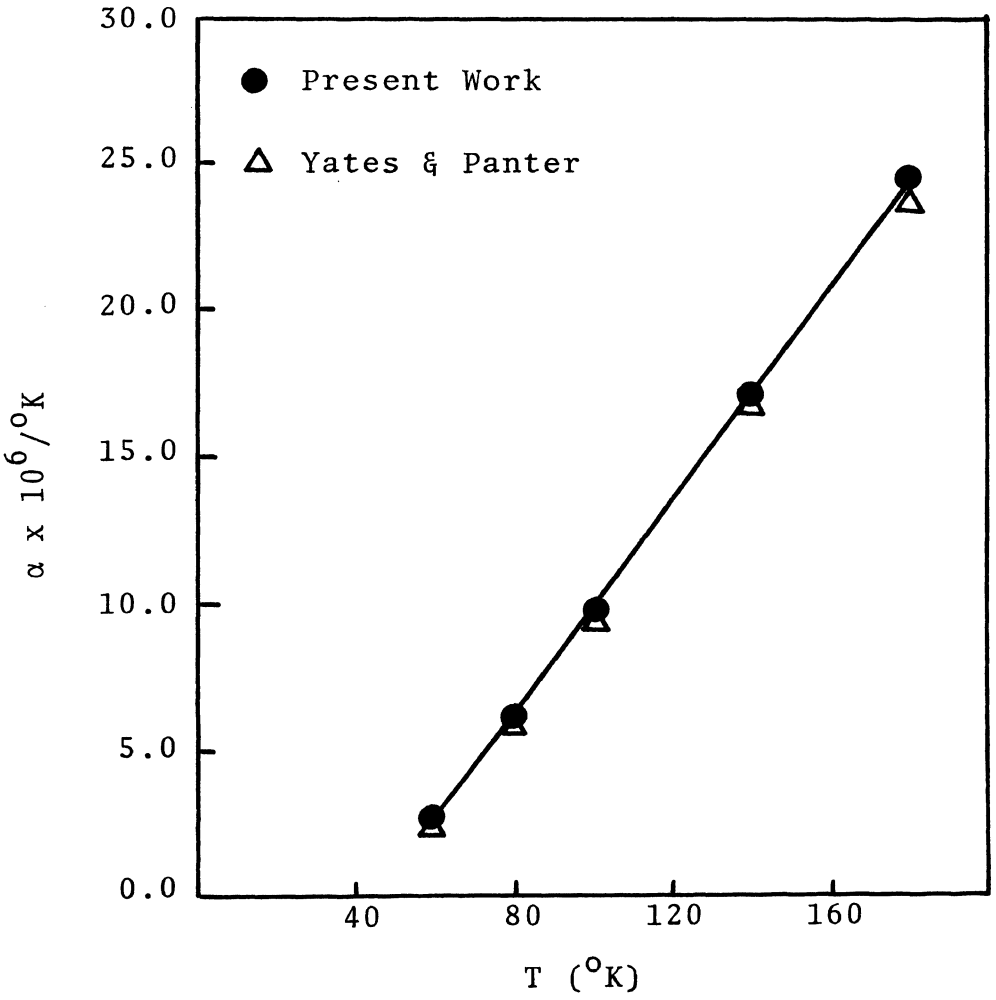

FIGURE 17. Thermal expansion of LiF

iii) It does not depend on the initial length, ℓ_o, or initial lattice parameter a_o; whereas, in the other method, it is $\Delta\ell/\ell_o$ for which they claim very high sensitivity (10^{-10}). The accuracy with which ℓ_o is known is, however, quite low. In the X-ray method a_o for $\Delta a/a_o$ is known very precisely.

iv) The X-ray method uses a small quantity (.05 gm) of a powder specimen which is easier to cool to a particular temperature and maintain it without excessive thermal gradients.

This is a severe problem in the other methods where the samples are large.

Thus, the dilatometric methods may be of higher sensitivity or precision but really of lower aboslute accuracy, concerning the expansion of the sample itself. Nevertheless, generally the thermal expansion data obtained in this investigation are in fairly good agreement with those published.

1. Chromium

The Grüneisen parameters of chromium decrease with temperature as predicted by the theory. This means that the amount of anharmonic contributions to the lattice vibrations of chromium is decreasing with temperature. No thermal anomaly is found in the vicinity of 120°K which could account for the

compressibility anomaly at 120°K found by Bolef and Klerk,[15] and the neutron diffraction data obtained by Shirane and Takei.[34] It is quite possible that the changes at 120°K in the lattice expansion, caused by the transition between two different states of antiferromagnetic ordering, is too small to be detected by our method where the sensitivity $\Delta a/a$ is about 2×10^{-6}.

2. Tungsten

The thermal expansion coefficients found in the present work are significantly different from those of the previous researchers. This disagreement may be due to the fact that they have used bulk samples obtained by compacting and sintering of tungsten powder.[49] Such bulk samples never attain the theoretical density[50] in contrast to molten metals, for example: iron.[51] No anomaly was found in the thermal expansion of tungsten in the 200°-140°K range as stipulated by Featherston and Neighbors.[38] The basis of their prediction of this thermal expansion anomaly is the anomalous bulk modulus behavior found by them for b.c.c transition metals Ta, W and Mo. They propose a transition between two different states of antiferromagnetic ordering. Shull and Wilkinson[52] studied the magnetic structures of W, Nb and Mo finding no evidence of

either aligned or unaligned moments on atoms. The Grüneisen parameter of W decreases with temperature as predicted by the theory.

3. Copper and nickel

For both of these metals, the thermal expansion data obtained are in excellent agreement with the published data. The Grüneisen parameters of Cu and Ni are almost constant in the temperature range of 180^{o}-40^{o}K with a slightly increasing trend at lower temperatures, but this cannot be emphasized much because the Grüneisen parameters are very sensitive to slight errors in the thermal expansion, specific heats and the bulk modulus data.

4. Iron

Effects of impurities on the thermal expansion behavior of iron cannot be really established from the present work since the changes in lattice parameters of iron samples of different purities are too small and in some cases within the limits of error. However, it seems that the influence of impurities on the lattice parameter decreases with decreasing temperatures. The thermal expansion coefficients obtained presently are in good agreement with the previous work. The Grüneisen parameters in the 180^{o}-40^{o}K range are constant.

5. Al_2Au

The lattice parameter and thermal expansion decrease with temperature without any anomalies. The expansion coefficients of Al_2Au are smaller than those of the metals constituting it, for example: $\alpha x10^6$ at 180^oK for Al is 19.0 and for Au it is 13.1 as compared to 9.3 for Al_2Au. But this is to be expected for an intermetallic compound where the interatomic bonding is strong and the substance is mechanically very hard.

6. LiF

Lattice parameters and thermal expansion coefficients decrease with temperature. For alkali halides, the variation in the Grüneisen parameter is expected at temperatures below $0.3\theta_D$, where θ_D is the Debye temperature.[2] For LiF $\theta_D=740^oK$, thus below 230^oK some variation in the Grüneisen parameter should be expected. But our results are contrary to this theory since the Grüneisen parameter of LiF has constant values within limits of error in the 180^o-40^oK range. It appears rather strange that the low temperature limit of Grüneisen parameter for LiF is already attained at or above 200^oK.

VI. THERMAL VARIATION OF LATTICE PARAMETERS OF SOME MAGNETIC INTERMETALLIC COMPOUNDS AND ITS CORELATION TO THEIR UNUSUAL MAGNETIC PROPERTIES

The thermal variation of lattice parameters of several magnetic intermetallic compounds was studied in the temperature range of 25^{o}-900^{o}K. These compounds were the following: Lu_2Fe_{17}, Y_2Fe_{17}, Y_2Co_{17}, α-Gd_2Fe_{17} having the hexagonal Th_2Ni_{17}-type structure, β-Gd_2Fe_{17} of the rhombohedral Th_2Zn_{17}-type structure and YCo_5, YNi_5 of hexagonal $CaCu_5$-type structure.

A. Literature Survey:

No thermal expansion data for these compounds were available. However, an immense amount of magnetic and crystallographic structure data do exist for these materials. Givord[57] has shown that the R_2M_{17}-type structure (R=rare earth or yttrium, M=transition metal) can be easily built from the $CaCu_5$-type building block by the following scheme:

$$3RM_5 - R + 2M = R_2M_{17}$$

One larger rare earth atom is substituted by two smaller transition metal atoms. If the substitution taken place as AB AB AB ..., the hexagonal Th_2Ni_{17}-type structure is obtained; whereas, ABC ABC ABC kind of substitution gives rise to Th_2Zn_{17}-rhombohedral structure (Fig. 18). The M-M (transition metal to

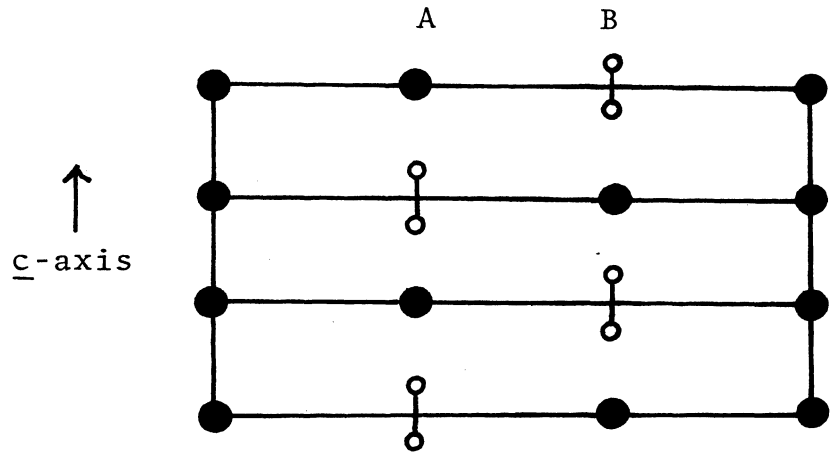

AB AB type of substitutional ordering in the hexagonal Th_2Ni_{17}-type structure

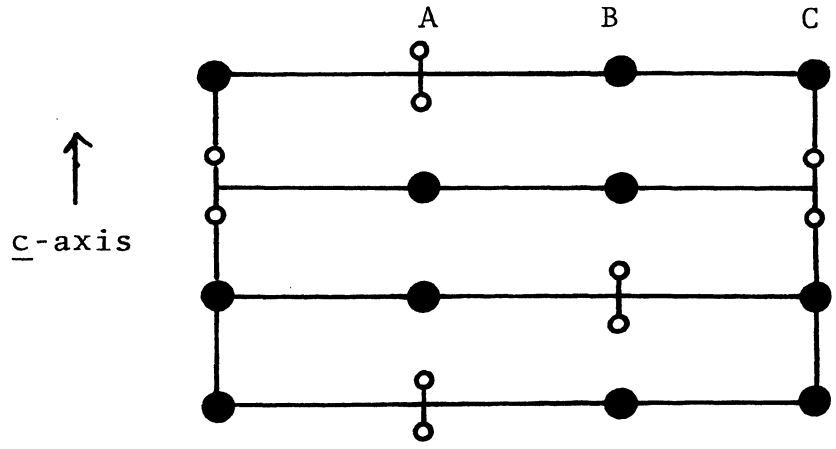

ABC ABC type of substitutional ordering in the rhombohedral Th_2Zn_{17}-type structure

● Rare-earth atom Pair of transition metal atoms

FIGURE 18. Schematic representation of substitutional ordering in the Th_2Ni_{17}(hex.) and Th_2Zn_{17} (rhomb.) structures

transition metal) interatomic distance for the substitution zone in these compounds is much shorter than that in the pure transition metals.[58] For instance, in the Lu_2Fe_{17} compound, the Fe-Fe interatomic distance in the substitution zone is 2.4 Å as compared to the 2.54 Å distance of closest approach in pure α-Fe.

Magnetic moments of transition metal atoms in these compounds have been measured from saturation magnetization data which are confirmed by neutron diffraction studies.[57,59] For Co and Ni compounds the magnetic moment of the transition metal atoms decreases very rapidly with increasing content of yttrium. Concurrently, their Curie temperatures, T_C, also decrease with increasing yttrium content. This is attributed to the fact that the conduction electrons of yttrium gradually fill up the 3d shells of Co or Ni. Thus, the magnetic moment decreases as the amount of yttrium content increases. No such regular behavior is found for Fe compounds. The Curie temperatures or the magnetic ordering temperatures of these compounds are as follows:[57,59]

	Y_2Fe_{17}	Lu_2Fe_{17}	Gd_2Fe_{17}	Y_2Co_{17}	Y_2Ni_{17}	YCo_5	YNi_5
T_C °K	310°	270°	479°	1000°	150°	900°	~

The Lu_2Fe_{17} compound has a peculiar magnetic behavior.[60,61] It is ferromagnetic up to 100°K and

becomes metamagnetic as the temperature increases, the magnetic ordering temperature being 270°K. A hysteresis is observed for the thermal magnetization studies. Neutron diffraction patterns at 77°K and also above the ordering temperatures show the same diffraction peaks, confirming the ferromagnetic nature of this compound at low temperatures. Magnetic moments are perpendicular to the c axis.

A new diffraction peak appears between 100°K and 270°K at a low angle when the temperature is decreased. In the same temperature range, two satellite peaks, (101^{+}) and (101^{-}) were observed on both sides of the (101) peak. These results are typical of a helical spin configuration where the screw axis is the c axis. The magnetic structure is, therefore, formed by ferromagnetic layers perpendicular to the c axis. The angle between the moments in the two consecutive layers varies from 12° at 110°K to 19° at 270°K. So there is a ferromagnetic to helimagnetic transition in this Lu_2Fe_{17} compound at about 100°K. Givord, et al.[57] explained this transition in terms of the distance dependence of interaction energy as proposed by Néel.[62]

B. Experimental Details:

All of the samples used in this investigation were kindly provided by Dr. R. Lemaire, C.N.R.S., Grenoble, France. All compounds were prepared by melting the

elements in a high-frequency levitation furnace and then homogenized at 1100°C for 3 days. Thermal variation of lattice parameters of these compounds were carried out by the powder diffraction method. Below 300°K the symmetrical back-reflection focusing camera, described previously, was used. For these measurements, the powders were ground in a boron nitride mortar and then were sieved through a special 20μ sieve. These gave reasonably adequate powder patterns. For exposures in the vicinity of room temperature, the camera with asymmetric loading features was used.[63] The powder samples were mounted on a quartz fiber. Hot or cold liquids (water + antifreeze) were circulated around this camera in a well-insulated aluminum jacket to produce temperatures in the range 250°-330°K. For temperatures higher than 330°K up to 900°K, a modified and redesigned Rigaku-Denki high temperature camera, as described previously, was used. Powder samples were mounted in quartz capillaries and sealed under vacuum. Chromium K_α radiation ($\lambda\alpha_1$=2.28962 Å) was used throughout the entire investigation. Lattice parameters were calculated by measuring the distance between the (600) α_1 and (300) α_1 lines as outlined in the sample calculations (Section III).

C. **Results**:

YCo_5 and YNi_5 (hexagonal $CaCu_5$-type) exhibit,

without any anomalies, normal thermal variation of lattice parameters (Fig. 19). These are also listed in Table XIX.

TABLE XIX

LATTICE PARAMETERS* OF YNi_5 AND YCo_5

T°K	YNi_5		YCo_5	
	a(Å)	c(Å)	a(Å)	c(Å)
40°	4.8714	3.9610	4.9360	3.9730
70°	4.8714	3.9610	4.9360	3.9730
100°	4.8714	3.9610	4.9370	3.9740
140°	4.8720	3.9614	4.9380	3.9740
180°	4.8760	3.9620	4.9390	3.9750
298°	4.8791	3.9697	4.9478	3.9760
373°	4.8820	3.9740	4.9520	3.9774
470°	4.8890	3.9780	4.9580	3.9810
650°	4.8890	3.9840	4.9710	3.9820
740°	4.9040	3.9900	4.9770	3.9840
900°	4.9160	3.9950	4.9850	3.9850

* Not corrected for refraction

Lattice parameters of Y_2Fe_{17}, Y_2Co_{17} and Y_2Ni_{17} are plotted in Fig. 20 (a-axis) and Fig. 21 (c-axis). For Y_2Co_{17} and Y_2Ni_{17} one again observes a normal behavior, i.e., only the lattice contributions to the thermal expansion. Y_2Fe_{17} shows an anomalous behavior

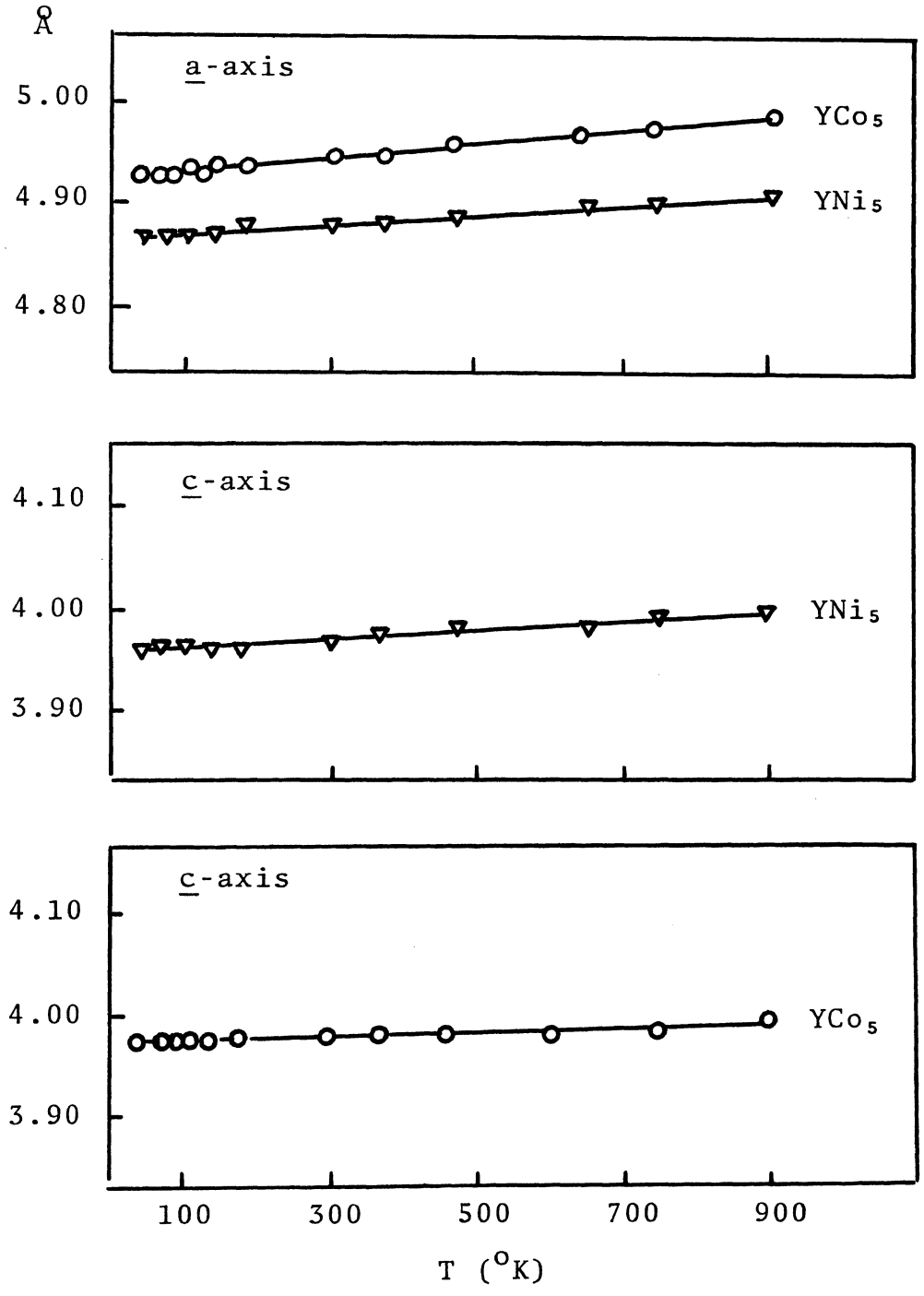

FIGURE 19. Lattice parameters of YCo_5 and YNi_5

below its Curie temperature (310°K): The c parameter (Fig. 21) increases as the temperature decreases below the magnetic ordering temperature while the a parameter (Fig. 20) does not change. Thus, for Y_2Fe_{17} there is a large negative thermal expansion in the c-direction below its magnetic ordering temperature. A similar anomalous thermal variation of lattice parameters of the iron compounds Lu_2Fe_{17} and α-Gd_2Fe_{17} was observed as shown in Fig. 22 (a-axis) and Fig. 23 (c-axis) along with the results for Y_2Fe_{17} for the sake of comparison (β-Gd_2Fe_{17} polymorph also has the same thermal expansion characteristics). Similar to Y_2Fe_{17}, Gd_2Fe_{17} and Lu_2Fe_{17} compounds show a large increase in their c parameters below their magnetic ordering temperatures (480°K for Gd_2Fe_{17} and 270°K for Lu_2Fe_{17}). Once again the a parameter changed very little below the magnetic ordering temperatures. The numerical values of the lattice parameters of Y_2Fe_{17}, Lu_2Fe_{17}, Gd_2Fe_{17} and Y_2Ni_{17} are listed in Tables XX, XXI, XXII, XXIII and XXIV, respectively.

No thermal hysteresis for the lattice parameters of Lu_2Fe_{17} was observed within the limits of our experimental accuracy (±.002 Å).

D. Discussion:

The thermal variation of the lattice parameters of the compounds studied in this section can be directly

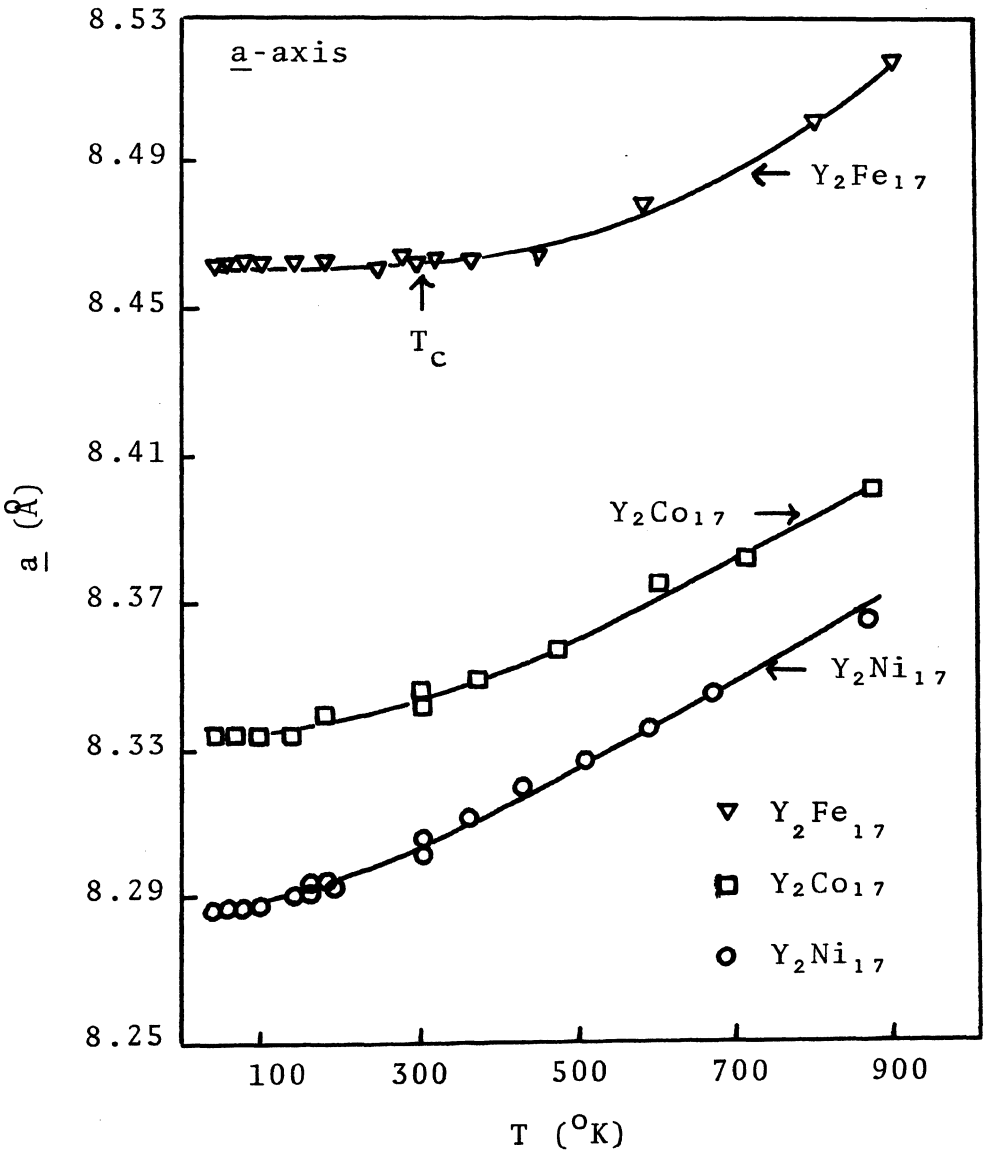

FIGURE 20. a-parameters of Y_2Fe_{17}, Y_2Co_{17} and Y_2Ni_{17}

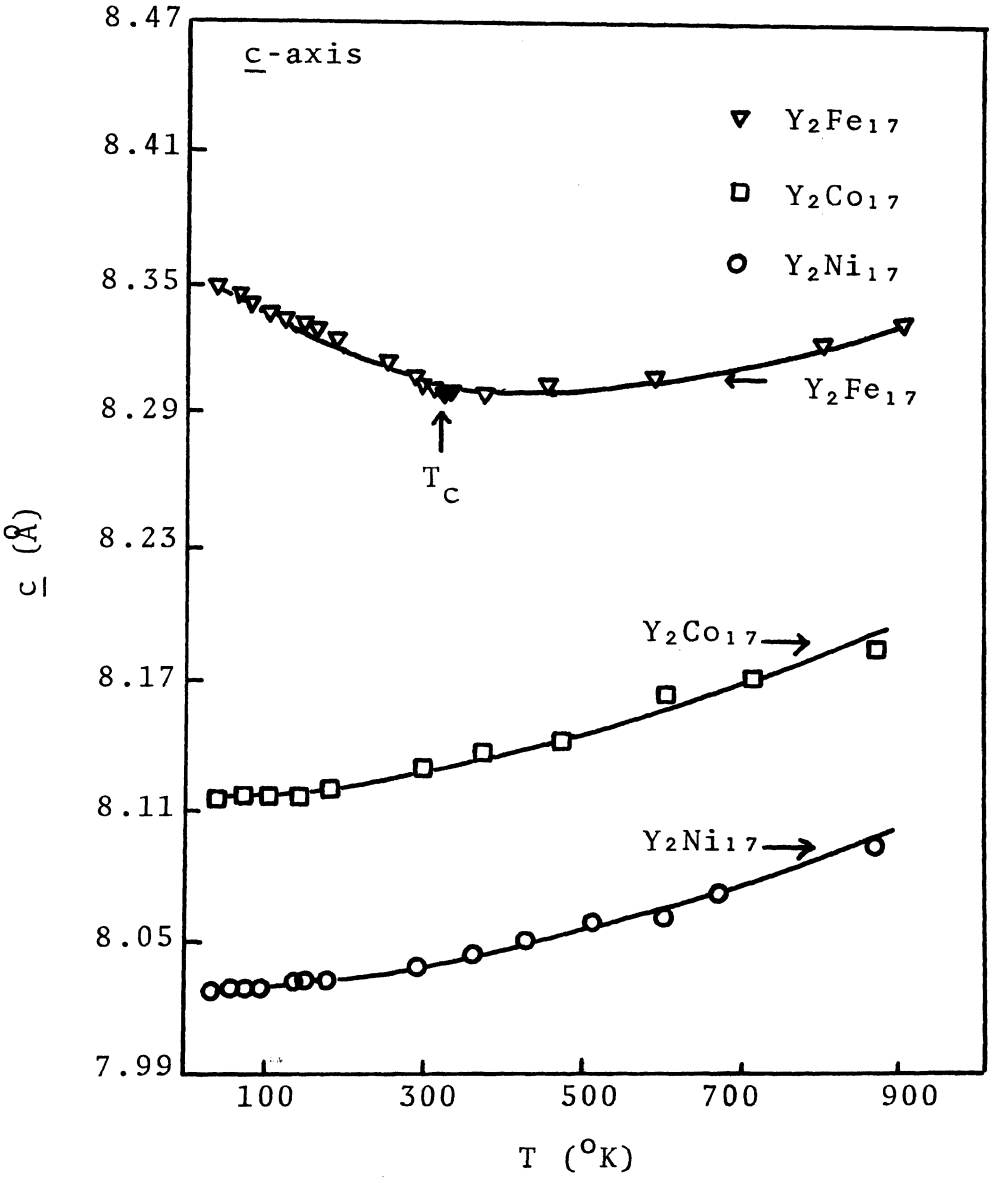

FIGURE 21. c-parameter of Y_2Fe_{17}, Y_2Co_{17} and Y_2Ni_{17}

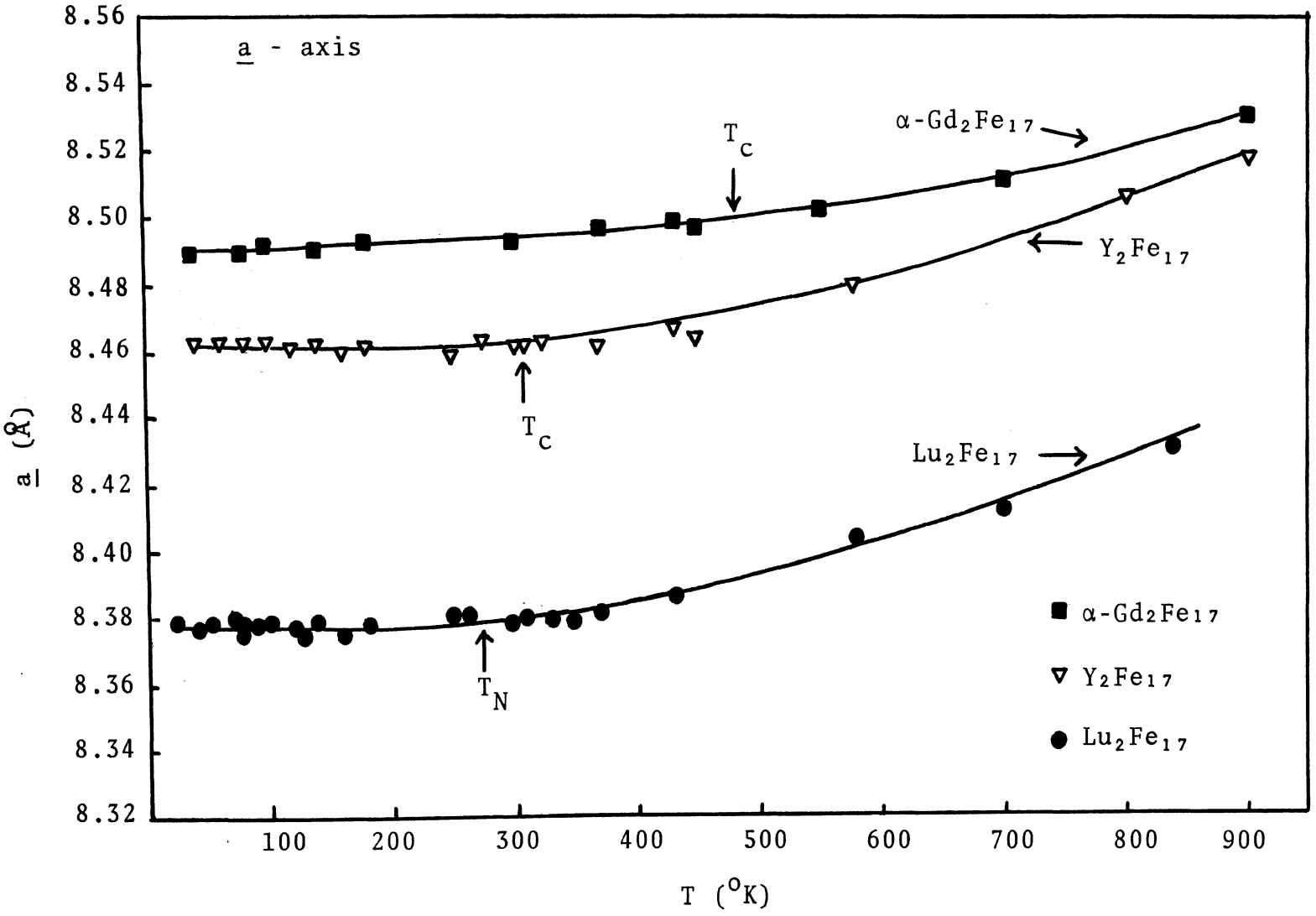

FIGURE 22. a-parameters of α-Gd_2Fe_{17}, Y_2Fe_{17} and Lu_2Fe_{17}

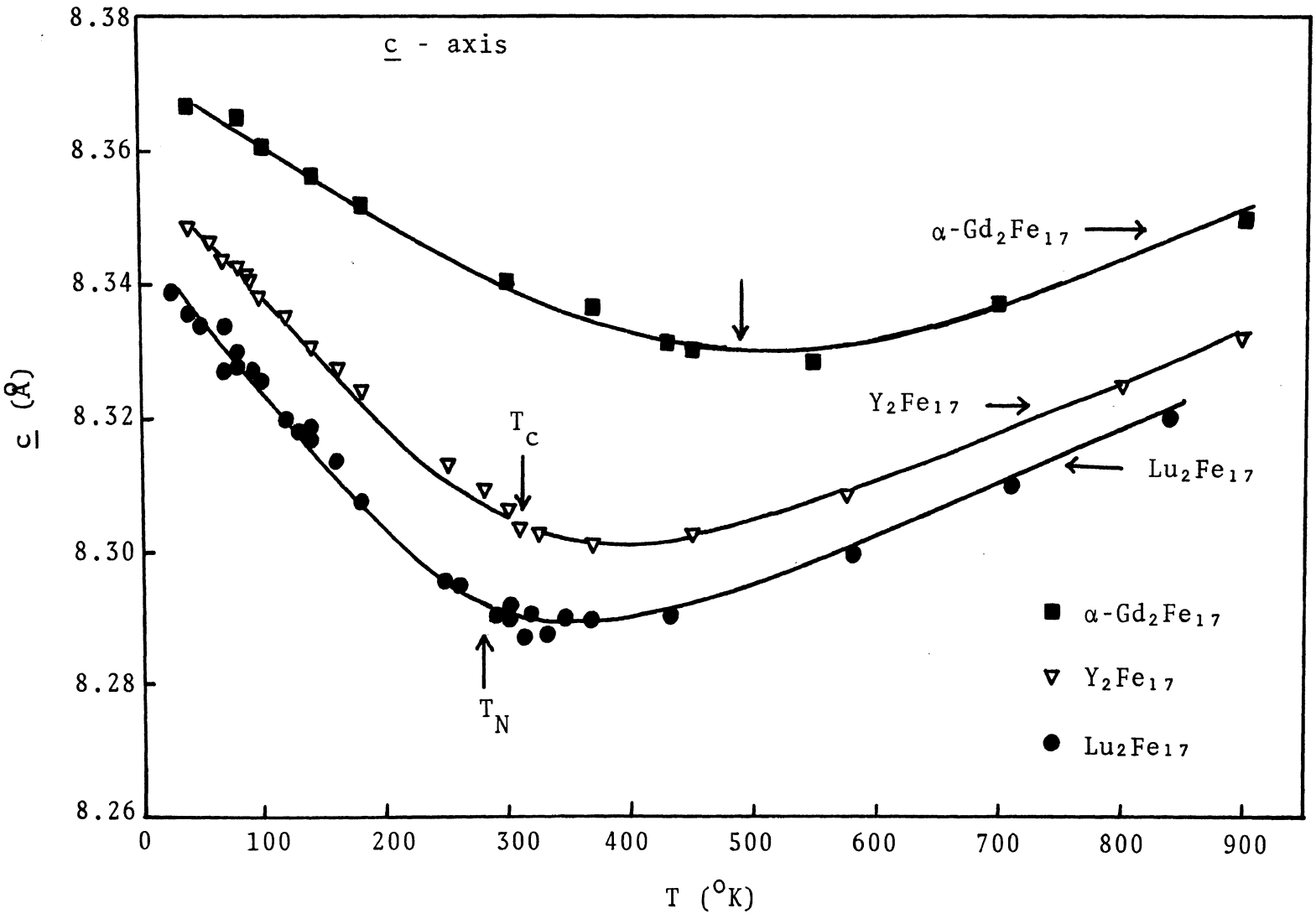

FIGURE 23. c-parameters of α-Gd_2Fe_{17}, Y_2Fe_{17} and Lu_2Fe_{17}

TABLE XX

LATTICE PARAMETERS* OF Y_2Fe_{17} COMPOUND

$T^{\circ}K$	a (Å)	c (Å)
40°	8.4620	8.3477
60°	8.4620	8.3455
80°	8.4620	8.3415
100°	8.4620	8.3375
120°	8.4620	8.3352
140°	8.4620	8.3300
160°	8.4620	8.3267
180°	8.4622	8.3235
252°	8.4580	8.3134
278°	8.4632	8.3081
298°	8.4622	8.3060
308°	8.4621	8.3035
323°	8.4625	8.3029
373°	8.4612	8.3010
453°	8.4641	8.3025
583°	8.4800	8.3075
803°	8.5061	8.3239
900°	8.5179	8.3319

* Not corrected for refraction

TABLE XXI

LATTICE PARAMETERS* OF Lu_2Fe_{17} COMPOUND

T°K	a (Å)	c (Å)
25°	8.3787	8.3377
40°	8.3772	8.3415
50°	8.3782	8.3340
70°	8.3795	8.3337
80°	8.3772	8.3297
90°	8.3781	8.3268
100°	8.3791	8.3278
120°	8.3777	8.3197
130°	8.3746	8.3181
140°	8.3786	8.3192
160°	8.3753	8.3144
180°	8.3786	8.3082
250°	8.3804	8.2959
264°	8.3799	8.2954
287°	8.3787	8.2911
298°	8.3796	8.2914
313°	8.3793	8.2871
330°	8.3798	8.2882
373°	8.3845	8.2900
433°	8.3905	8.2903
583°	8.4084	8.3001
708°	8.4169	8.3099
843°	8.4346	8.3197

* Not corrected for refraction

TABLE XXII

LATTICE PARAMETERS* OF α-Gd_2Fe_{17} COMPOUND

$T^{\circ}K$	a (Å)	c (Å)
40°	8.4855	8.3660
80°	8.4867	8.3640
100°	8.4879	8.3620
140°	8.4879	8.3560
180°	8.4901	8.3540
298°	8.4945	8.3409
373°	8.4992	8.3370
433°	8.4992	8.3320
453°	8.4992	8.3312
553°	8.4996	8.3290
693°	8.5127	8.3373
903°	8.5308	8.3500

* Not corrected for refraction

TABLE XXIII

LATTICE PARAMETERS* OF Y_2Co_{17} COMPOUND

T°K	a (Å)	c (Å)
40°	8.3291	8.1190
70°	8.3291	8.1190
100°	8.3291	8.1190
140°	8.3295	8.1203
180°	8.3400	8.1220
298°	8.3462	8.1342
373°	8.3490	8.1380
473°	8.3566	8.1430
600°	8.3753	8.1643
713°	8.3820	8.1707
870°	8.4043	8.1841

* Not corrected for refraction

TABLE XXIV

LATTICE PARAMETERS* OF Y_2N_{17} COMPOUND

T^oK	a (Å)	c (Å)
40^o	8.2865	8.0268
60^o	8.2865	8.0268
80^o	8.2865	8.0268
100^o	8.2867	8.0278
140^o	8.2900	8.0314
180^o	8.2930	8.0320
298^o	8.3062	8.0409
363^o	8.3115	8.0459
433^o	8.3199	8.0506
513^o	8.3270	8.0565
593^o	8.3357	8.0626
673^o	8.3450	8.0724
873^o	8.3651	8.0947

* Not corrected for refraction

related to their magnetic properties and crystallographic structures.

Since the YNi_5 and YCo_5 compounds possessing the building block structure ($CaCu_5$) of the R_2M_{17} compounds do not show any thermal expansion anomalies, the anomalous thermal expansion and magnetic properties of the Fe compounds cannot be related to their building block structure.

R_2Co_{17} and R_2Ni_{17} compounds behave very differently from the R_2Fe_{17} compounds. These Co and Ni compounds do not show any thermal expansion anomalies; whereas, all of the R_2Fe_{17} compounds studied in this investigation show a large negative thermal expansion along the c-axis below their magnetic ordering temperatures. These results indicate that for the Co and Ni compounds the magnetic properties are mainly dependent on the conduction electron transfer from the yttrium atom to the 3d shell of Co or Ni, gradually filling their 3d shells. However, for the Fe compounds, it is apparent that the magnetic properties are mainly determined by the Fe-Fe interatomic distances and number of Fe nearest neighbors in the crystal.

The anomalous thermal expansion of R_2Fe_{17} type compounds can be understood in terms of magnetic interactions in the crystals as follows: These Fe compounds are ferromagnetic so the magnetic interactions on the whole are positive. This forces the

magnetic moments to be parallel everywhere, even in the substitution zone where the Fe-Fe interatomic distance is very short (2.4Å). Due to these short Fe-Fe interatomic distances in the substitution zone, there is an overlap of the 3d wave functions of Fe atoms, giving rise to negative direct interactions in the substitution zone. These negative magnetic interactions remain unsatisfied since the magnetic moments have to be parallel in the substitution zone as explained before. Hence, there is a large amount of magnetic energy stored in this substitution zone. This stored energy can be minimized or relieved if the negative magnetic interactions can decrease. This is exactly what happens when the c parameter increases. Now, as the temperature further decreases, the magnetization of Fe increases and the stored energy increases. Accordingly, once again for the minimization or relief of this stored energy, the c parameter increases. Thus, there is a continuous increase in the c parameter as these Fe compounds are cooled below their magnetic ordering temperature. Since this anomalous thermal expansion is observed for both the polymorphic forms, hexagonal α-Gd_2Fe_{17} and rhombohedral β-Gd_2Fe_{17}, where the only difference is the type of substitutional ordering, the anomalous thermal expansion seems only to be a function of the Fe-Fe interatomic distances in the substitution zone and their magnetic interactions.

The ferromagnetic to helimagnetic transition for Lu_2Fe_{17} compound as observed by Lemaire and Givord can also be explained along similar lines of reasoning as above. Due to the lanthanide contraction in the rare-earth metals series, Lu has the smallest atomic radius and since the rare-earth forms the skeleton of the structure, the Fe-Fe interatomic distances in the substitution zone are much shorter. As mentioned before, there is an overlap of 3d wave functions of Fe atoms in the substitution zone giving rise to negative magnetic interactions. These negative magnetic interactions are strong enough to stabilize the helical spin configuration. But even in the helical configuration the magnetic moment in the substitution zone are not entirely anti-parallel. Once again large amounts of magnetic energy are stored in the substitution zone. As the magnetic ordering increases with decreasing temperature to minimize the stored energy, the $\underline{c}$ parameter increases. At the transition the negative direct interactions are no longer strong enough to stabilize the helical spin configuration and as a result the compound Lu_2Fe_{17} becomes ferromagnetic with the temperature decrease. Obviously no such transition is observed in Y_2Fe_{17}, since the atomic radius of Y is much larger than that of Lu and, hence, it can only stabilize the ferromagnetic configuration. A similar helimagnetic-ferromagnetic transition should be observed

in the other R_2Fe_{17} compounds where the rare-earth atoms have small atomic radius, for example, in Tm_2Fe_{17} and Yb_2Fe_{17} compounds. Ce_2Fe_{17} compound should show such a transition because here Ce has a very small atomic radius since Ce is in the tetravalent state.

In conclusion, the number of Fe nearest neighbors and their interatomic distances play a major role in determining the magnetic properties of R-Fe compounds. In the analogous R-Co compounds, the magnetic properties are determined by conduction electron transfer from the rare-earth to Co whose 3d electrons are less strongly bound. These two different behaviors should lead to an Fe-Co ordering in the R-Fe-Co ternary compounds reinforcing the magnetocrystalline anisotropy. Further studies in this direction will be of great interest in developing permanent magnets.

VII. FUTURE STUDIES AND THE PROPOSED NEW DESIGN OF A BETTER AND MORE VERSATILE CAMERA

A. Future Studies:

From the present investigation, it seems to follow that a careful thermal expansion of the two isotopes of Si (28 and 30) should lead to a better understanding of the anomalous thermal expansion of this element. If the phonon spectrum is really causing this effect, changing the mass of the vibrating atoms should give an idea as to what are the major factors involved. Similarly, the study of Si-Ge alloys in this direction would also be helpful.

The effects of impurities on the thermal expansion of solids at low temperatures remains in doubt. Careful studies of metal samples of various purities (knowing the elements present) should prove informative.

For the R_2Fe_{17} magnetic intermetallic compounds, when the exact crystal structure is known, one should be able to develop the theory concerning the exact nature of the exchange interactions in similar compounds and their relation to the anomalous thermal expansion in these crystals. Thermal expansion studies on Ce_2Fe_{17}, Tm_2Fe_{17} and Yb_2Fe_{17} should shed more light on the ferromagnetic-helimagnetic transition such as observed in Lu_2Fe_{17}. Also, the thermal expansion and neutron diffraction studies on the ternary R-Fe-Co alloys will

be interesting from the point of view of Fe-Co ordering in these compounds.

B. Proposed New Design of the Low Temperature Camera:

The low temperature camera used in this investigation has the following limitations:

i) In this symmetrical back-reflection focusing camera design, the sample rotation or oscillation is not possible. Thus, one has to use powders with particle size of <20μ to obtain sharp and uniform lines for precise thermal expansion studies. It is exceedingly difficult to obtain 20μ powders of some materials, especially of softer metals, easily oxidizable metals or pyrophoric materials.

ii) The "Cryomite" or the Joule-Thompson pump used to cool the sample is only capable of going down to 25°K. Sometimes data below this temperature are needed and cannot be obtained.

In view of the above limitations of the present design, a wide variety of refrigerating systems and cameras were reviewed to develop a better and more versatile camera. At the present time the "Cryo-Tip" (Model LT-3-110B) cooling system made commercially by Air Products, Inc., Allentown, Pa. seems to be the most suitable. This system has the following advantages and

features:

i) It has the capability of continuous cooling from 300°K to 2°K with minimum space and support requirements.

ii) However, it uses liquid He, H_2, N_2, O_2, etc. for cooling. Liquid gas flow is controlled by a micrometer needle valve. A heater at the cold head permits experiments up to 300°K. The cool down time to 2°K is about 15 minutes, but this can be variable depending on the heat load (size of sample) on the cold head.

iii) Operates in any position which is very suitable for future design changes. Remote liquid storage container and flexible transfer lines facilitate the design of camera around the cold head.

iv) The vacuum shroud to the cooling unit joint is rotatable and thus sample rotation is possible, and a convenient particle size powder can be used for the thermal expansion studies.

v) Uses about ½ liter/hour of liquid He for experiments below 20°K. Liquid He consumption is, therefore, low enough for the experiments to be feasible at reasonable costs.

Temperature measurements will be made as follows:

i) An Fe-doped gold versus chromel thermocouple will

be mounted on the cold head, and its output in millivolts will be measured by a Leeds and Northrup potentiometer. This thermocouple has a larger temperature sensitivity range and will be carefully calibrated.

ii) Two temperature sensitive resistance sensors will also be mounted on the cold head near the sample holder. These sensors will be calibrated by the supplier. For the temperature range of $300^{o}K$-$40^{o}K$, a platinum resistance sensor will be used and for the temperature below $40^{o}K$ to $2^{o}K$, the germanium resistance sensor since the sensitivity of the platinum resistance sensor is insufficient below $40^{o}K$. The output from these sensors in resistance will be measured on the presently existing resistance measuring system, "Cryodial," supplied by the Malaker Corporation of High Bridge, New Jersey.

With these two independent measurements of temperature, one can achieve a capability of $\pm 0.1^{o}K$ in the temperature measurement.

The vacuum shroud surrounding the cold head shall have the following features so as to make the system most versatile:

i) The vacuum shroud will be made of stainless steel, and it will be bakeable to remove any adsorbed

gases from the shroud walls.

ii) It will have adequate radiation shields.

iii) It will have two slits covered with Be sheet, each of them as shown in Fig. 24. These beryllium slits or windows are necessary for the diffracted X-rays to strike the film outside the shroud. The X-ray beam will enter and exit through the Mylar windows. A copper sample holder will be designed which can be screwed on the cold head. On the center of the sample holder will be a thin wire of copper or any other suitable heat conductive material as a powder support. Powder to be investigated will be mounted to this wire by high thermal conductivity low temperature cement transparent to X-rays. The sample holder will be rotated with the cooling system. An asymmetrically loaded film will be placed around the shroud in a light tight film cylinder. One has essentially the Straumanis geometry which eliminates the film shrinkage errors and no exact knowledge of the camera radius is needed. The sample can be aligned properly by a microscope since the sample holder can be detached from the cold head easily. This whole arrangement is shown in Fig. 24. The prime advantage of this setup is that it is capable of giving full asymmetric patterns with front and back reflections. For many organic,

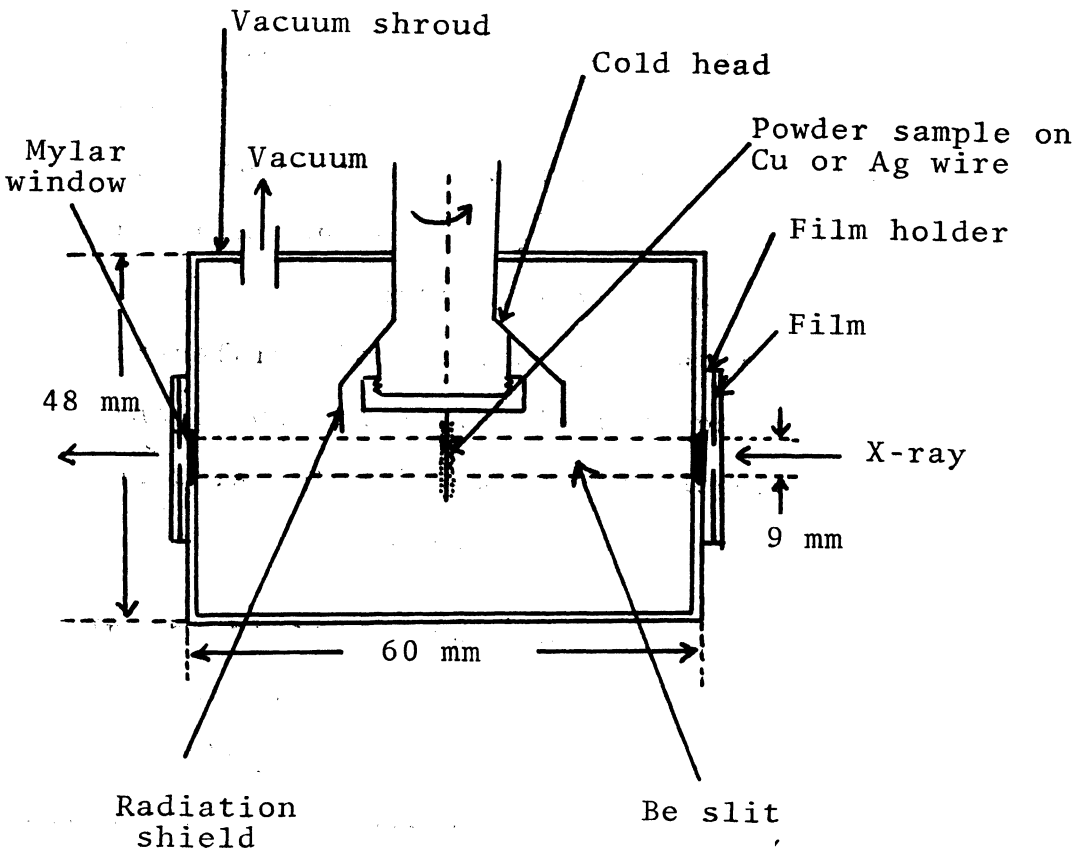

FIGURE 24. Low temperature X-ray diffraction camera (Straumanis arrangement)

organo-metallic and polymeric compounds only the front reflections are present, and in that case the back reflection region of the film will be empty. A single crystal can also be mounted on the copper fiber and the rotating crystal pattern can be easily obtained at low temperatures. This can be particularly useful if a phase transformation at low temperatures is suspected. The precision of the lattice parameters obtained in this setup is quite high depending upon the accuracy of temperature control.

In the bottom of the same vacuum shroud, a Be slit with a Mylar window will be mounted in the center of the bottom of the shroud. This arrangement will deliver X-ray beams for a back-reflection pattern as shown in Fig. 25. The sample together with the cold head can be rotated permitting use of coarser particle size powders. Proper film shrinkage corrections can be made by means of knife edges or any other suitable means. Flat film geometry could be used with a multi-exposure cassette on a single film which is very useful for routine lattice expansion studies. A symmetrical back-reflection focusing camera geometry can also be provided for with the advantages of very sharp and uniform diffraction lines and short exposure times.

In conclusion, with this proposed design, the

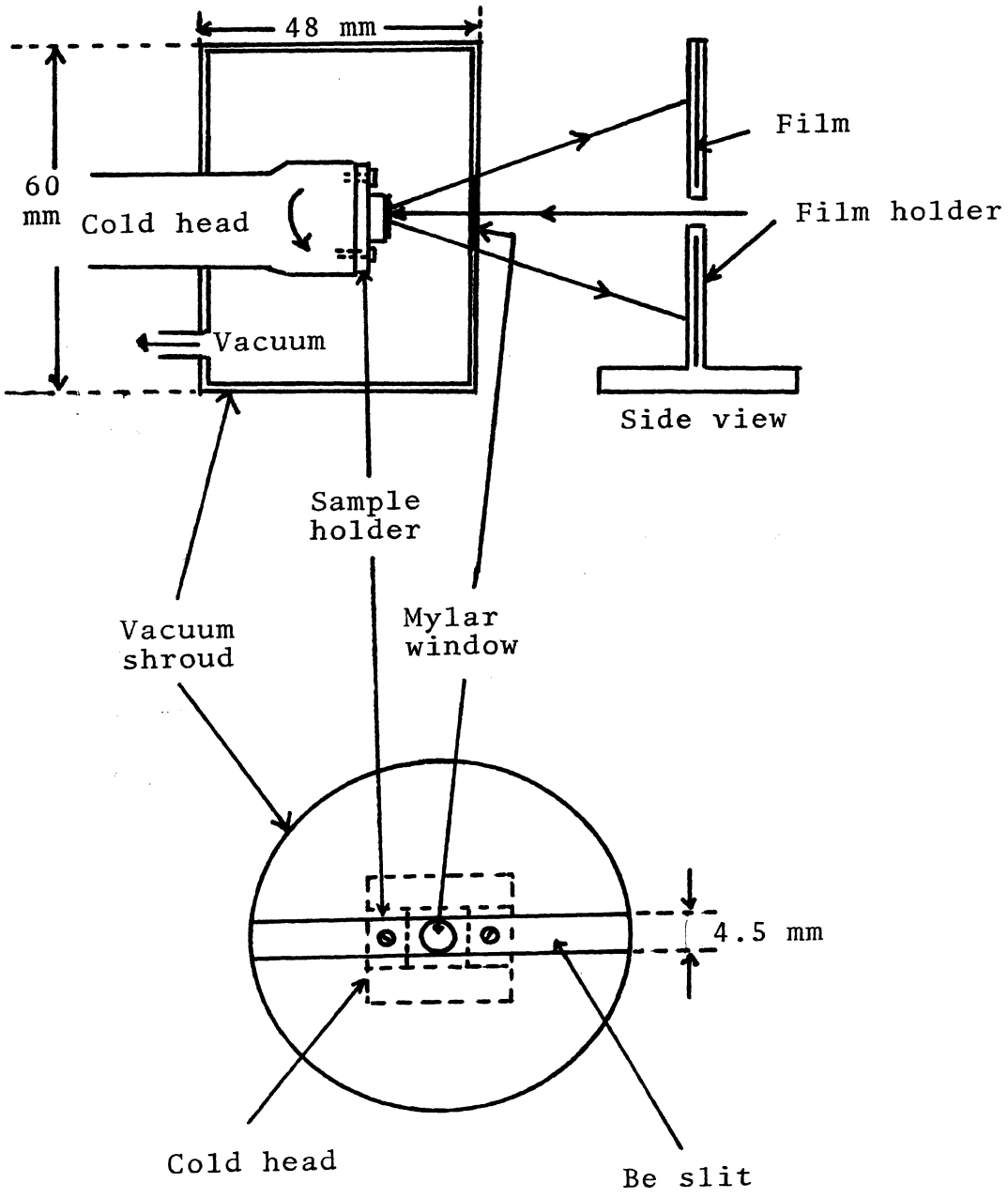

FIGURE 25. Back-reflection low temperature camera

lattice expansion study of any crystalline materials is possible. The very fine powder is not needed and temperatures as low as $2^{o}K$ can be achieved. Since the entire apparatus will be made of stainless steel and brass, thermal expansion studies of samples in magnetic fields are also possible. This opens an avenue to study magnetostriction as a function of magnetic fields and temperatures. The easy magnetization directions of ferromagnetic substances can also be found by performing the X-ray diffraction studies under a magnetic field. Since the powder particles will be aligned in preferred orientation (easy direction of magnetization) in the magnetic field, the intensity of some X-ray lines will increase and others decrease appreciably. Hence, the easy direction of magnetization can be deduced.

VIII. CONCLUSIONS

Thermal expansion studies of various types of solids have been carried out and these were corelated to their crystallographic structures and various properties.

Silicon shows a negative thermal expansion behavior below 120^{o}K. Intuitive arguments to explain this phenomenon are put forward and further studies have been proposed which may throw more light on this subject.

Diamond shows no thermal expansion anomalies despite the theoretical predictions. However, its thermal expansion is found to vary with temperature.

Any disagreements between the present results and the published data have been attributed to differences in the techniques employed and the types of samples used in these techniques.

Metals studied in this investigation show a normal thermal expansion behavior. The Grüneisen parameters of some of the metals have a slight tendency to increase as the temperature decreases. For tungsten a large difference is found between the present results and the published data. This is explained in terms of the lack of theoretical density data and the presence of microcracks, voids, inclusion and other defects present in the samples used by previous workers. No anomalies are found in the thermal expansion of tungsten in the 180-40^{o}K range contrary to the predictions by Featherston and Neighbors. Chromium also

is normal in its thermal expansion behavior without any anomalies at 120°K corresponding to a magnetic ordering effect. Ni, Cu and Fe behave as typical metals in their thermal expansion behavior at low temperatures. Effects of impurities on the thermal expansion of Fe at low temperatures seem to be negligible. The intermetallic compound $A\ell_2Au$ exhibits a much smaller thermal expansion than its constituents and this is explained in terms of its structure and interatomic bonding. The lattice parameters and thermal expansion coefficients for LiF are reported along with its Grüneisen parameters. In spite of the high Debye temperature of LiF, its Grüneisen parameters attain constant values at unusually high temperatures.

In the magnetic intermetallic compounds, an anomalous negative thermal expansion for R_2Fe_{17} compounds is observed. This is explained in terms of the magnetic interactions between the Fe atoms in the substitution zone. The R_2Co_{17} and R_2Ni_{17} compounds show a normal behavior in their thermal expansion. This difference between the Fe compounds on one hand and the Co and Ni compounds on the other hand is also explained in terms of their magnetic properties. The helimagnetic to ferromagnetic transition of Lu_2Fe_{17} is clearly related to the negative direct exchange in the substitution zone. Further studies for gaining better understanding of this transition are proposed.

A better and versatile low temperature X-ray camera design is proposed. The theoretical capability and actual construction of this camera are discussed in detail.

REFERENCES

1. Grüneisen, E., Ann. Phys., 39, 257 (1912).
2. Barron, T. H. K., Phil. Mag., 46, 720 (1955).
3. Blackman, M., Proc. Phys. Soc. B, 70, 827 (1957).
4. White, G. K., Prog. Low Temp. Phys., IV (New York: John Wiley & Sons, Inc., 1964).
5. Meincke, P. P. M. and Graham, G. M., Proc. VIII Int. Conf. Low Temp. Phys., London: Butterworths, 1963.
6. Shah, J. S. and Straumanis, M. E., to be published, J. Appl. Phys., Aug. 1971.
7. Glover, R. E., Z. Physik, 138, 222 (1954).
8. Gott, A., Ann. Physik, 41, 520 (1942).
9. Smith, R. C., Thesis, North Carolina State College, 1934.
10. Batchelder, D. N. and Simmons, R. O., J. Chem. Phys., 41, 2324 (1964).
11. Reeber, R. R. and Kulp, B. A., Trans. Met. Soc. AIME, 223, 698 (1965).
12. Rudman, R., J. Appl. Cryst., 2, 95 (1969).
13. Woodard, C. L. and Straumanis, M. E., to be published in J. Appl. Cryst.
14. Dolling, G. and Cowley, R. A., Proc. Phys. Soc., 88, 463 (1966).
15. Bolef, D. I. and Klerk, J. De., Phys. Rev., 129, 1063 (1963).
16. Givord, F. and Lemaire, R., J. less. Comm. Metals, 21, 463 (1970).
17. Mott, N. F. and Jones, H., The Theory of the Properties of Metals and Alloys (New York: Dover Publications, 1958) 15.
18. Varley, J. H. O., Proc. Phys. Soc., A237, 413 (1956).
19. White, G. K., J. Phys. Chem. Solids, 23, 169 (1962).

20. Woodard, C. L., Ph.D. Thesis, University of Missouri, pp. 12-32 (1968).

21. Lipson, H. S. and Wilson, A. J. C., J. Sci. Inst., 18, 144 (1941).

22. Lonsdale, K., International Tables for Crystallography, Vol. III (Birminham, England: Knyoch Press, 1962) 123.

23. Merryman, R. G. and Kempter, C. P., J. Am. Cer. Soc., 48, 202 (1964).

24. Gibbons, D. F., Phys. Rev., 112, 136 (1958).

25. Novikova, S. I. and Strelkov, P. G., Sov. Phys. S. State, 1, 1687 (1960).

26. Flubacher, P., Leddbetter, A. J. and Morrison, J. A., Phil. Mag., 4, 273 (1959).

27. McSkimm, H. J., J. Appl. Phys., 24, 988 (1953).

28. Thewlis, J. and Davey, A. R., Phil. Mag., Ser. 8, 1, 409 (1956).

29. Novikova, S. I., Fiz. Tverd. Tela., 2, 1617 (1960).

30. Parrish, W., Acta Cryst., 13, 838 (1960).

31. Fine, M. E., Griner, E. S. and Ellis, W. C., Trans. AIME, 191, 56 (1951).

32. White, G. K., Aust. J. Phys., 14, 359 (1961).

33. James, W. J., Straumanis, M. E. and Rao, P. B., J. Inst. Metals, 90, 175 (1962).

34. Shirane, G. and Takei, W. J., Proc. Int. Conf. Mag., Kyoto, J. Phys. Soc. Japan, 17, Suppl. B1-B3 (1961).

35. Corruccini, R. J. and Gniewek, J. J., NBS Monograph 21, Washington, D. C.: U. S. Dept. Commerce (1960).

36. Nix, F. C. and McNair, D., Phys. Rev., 61, 74 (1942).

37. Corruccini, R. J. and Gniewek, J. J., NBS Monograph 29, Washington, D. C.: U. S. Dept. Commerce (1961).

38. Featherston, F. H. and Neighbors, J. R., Phys. Rev., 130, 1324 (1963).

39. Bolef, D. I. and Klerk, J. De., J. Appl. Phys., 33, 2311 (1962).

41. Buffington, R. M. and Latimer, W. M., J. Am. Chem. Soc., 48, 2305 (1926).

42. Nix, F. C. and McNair, D., Phys. Rev., 60, 597 (1941).

43. Bijl, D. and Pullan, H., Physica, 21, 285 (1955).

44. Rubin, T., Altman, W. and Johnston, H. L., J. Am. Chem. Soc., 76, 5289 (1954).

45. Fraser, D. B. and Hallett, A. C. H., Proc. VIII Int. Conf. Low Temp. Phys., Toronto: University of Toronto Press, 689 (1961).

46. Allers, G. A., Neighbors, J. R. and Sato, H., J. Phys. Chem. Solids, 13, 40 (1960).

47. Rayne, J. A. and Chandrasekhar, B. S., Phys. Rev., 122, 1714 (1961).

48. Straumanis, M. E. and Chopra, K. S., Z. Phys. Chemie, 42, 344 (1964).

49. Parker, G. D., Mellor's Modern Inorganic Chemistry, (New York: John Wiley and Sons, Inc., 1967) 881.

50. Promisel, N. E., The Science and Technology of W, Ta, MO, Nb and Their Alloys (New York: McMillan Company, 1964) 466.

51. Straumanis, M. E. and Kim, C. D., Z. Metallkde, 60, 272 (1969).

52. Shull, C. G. and Wilkinson, M. K., Rev. Mod. Phys., 25, 100 (1953).

53. Himmler, U., Peisl, H., Sepp, A. and Waidelich, Siemens Review, 17, 33 (1970).

54. Yates, B. and Panter, C. H., Proc. Phys. Soc., 80, 373 (1970).

55. Clausius, K. and Eichenhomer, W., Z. Naturf., 42, 424 (1949).

56. Briscoe, C. V. and Squire, C. F., Phys. Rev., 106, 1175 (1957).

57. Givord, F., Ph.D. Thesis, University of Grenoble, France (1969).

58. Lemaire, R., Givord, D., James, W. J., Moreau, J. M. and Shah, J. S., Am. Cryst. Assoc., Winter Meeting, F-13 (1971).

59. Lemaire, R., Cobalt, 32, 132 (1966).

60. Givord, D., Givord, F. and Lemaire, R., J. de Physique, to be published.

61. Givord, D., Lemaire, R., James, W. J., Moreau, J. M. and Shah, J. S., Trans. IEEE, Magnetics, to be published, Sept. 1971.

62. Néel, L., Ann. Phys., 5, 232 (1936).

63. Straumanis, M. E., J. Appl. Phys., 20, 726 (1949).

VITA

Jayantkumar Shantilal Shah was born on April 22, 1944 in Rajkot, India. He received his primary and secondary education in Rajkot, India. He has received his college education from M. S. University of Baroda in Baroda, India and the University of Missouri-Rolla in Rolla, Missouri. He received a Bachelor of Science degree in geology from the M. S. University of Baroda in April 1964. He received a Bachelor of Science degree in Metallurgical Engineering from the University of Missouri-Rolla in January 1966.

He was employed as a Research Engineer with the Lindberg Corporation, Melrose Park, Illinois from January 1966 to August 1967.

He has been enrolled in the Graduate School of the University of Missouri-Rolla since September 1967 and has held the Teaching Assistantship for the period September 1967 to June 1968 and the Space Sciences Research Assistantship for the period July 1968 to June 1971.